CZECH TECHNICAL UNIVERSITY IN PRAGUE
FACULTY OF MECHANICAL ENGINEERING

MASTER THESIS

Design of small liquid propellants rocket engine

Michal Málek

Prague 2021

ZADÁNÍ DIPLOMOVÉ PRÁCE

I. OSOBNÍ A STUDIJNÍ ÚDAJE

Příjmení: **Málek** Jméno: **Michal** Osobní číslo: **459583**

Fakulta/ústav: **Fakulta strojní**

Zadávající katedra/ústav: **Ústav letadlové techniky**

Studijní program: **Letectví a kosmonautika**

Studijní obor: **Letadlová a kosmická technika**

II. ÚDAJE K DIPLOMOVÉ PRÁCI

Název diplomové práce:

Návrh malého motoru na kapalné pohonné látky

Název diplomové práce anglicky:

Design of small liquid propellants rocket engine

Pokyny pro vypracování:

1) Navrhněte malý experimentální raketový motor na dvousložkové kapalné pohonné látky
(Požadavky: kapalná alespoň jedna ze složek PL, tah motoru přibližně 100 N, primární určení jako demonstrátor pro statické testy)
2) Prověřte souhlas parametrů motoru stanovených analytickými výpočty s numerickými simulacemi
3) Stanovte požadavky na testovací stav pro tento motor

Seznam doporučené literatury:

G.P. Sutton, O. Biblarz, Rocket Propulsion Elements, Wiley, 9th ed., 2017, ISBN 978-1-118-75365-1
a další literatura dle doporučení vedoucího

Jméno a pracoviště vedoucí(ho) diplomové práce:

Mgr. Jaroslav Kousal, Ph.D., ústav letadlové techniky FS

Jméno a pracoviště druhé(ho) vedoucí(ho) nebo konzultanta(ky) diplomové práce:

Datum zadání diplomové práce: **30.04.2021** Termín odevzdání diplomové práce: **30.07.2021**

Platnost zadání diplomové práce: _____

Mgr. Jaroslav Kousal, Ph.D. podpis vedoucí(ho) práce	Ing. Robert Theiner, Ph.D. podpis vedoucí(ho) ústavu/katedry	prof. Ing. Michael Valášek, DrSc. podpis děkana(ky)

III. PŘEVZETÍ ZADÁNÍ

Diplomant bere na vědomí, že je povinen vypracovat diplomovou práci samostatně, bez cizí pomoci, s výjimkou poskytnutých konzultací. Seznam použité literatury, jiných pramenů a jmen konzultantů je třeba uvést v diplomové práci.

Datum převzetí zadání _____ Podpis studenta _____

Declaration

I declare that I have developed and written this Master thesis completely by myself, under the guidance of thesis supervisor Mgr. Jaroslav Kousal Ph.D. All sources used are declared in the list of literature.

In Prague…….. ……..

Anotační list

Jméno autora:	Michal Málek
Název práce:	Návrh malého motoru na kapalné pohonné látky
Anglický název práce:	Design of small liquid propellants rocket engine
Akademický rok:	2020/2021
Ústav:	Ústav letadlové techniky
Vedoucí práce:	Mgr. Jaroslav Kousal Ph.D.
Bibliografické údaje:	Počet stran: 67
	Počet obrázků: 53
	Počet tabulek: 4
	Počet příloh: 1 CD
Klíčová slova:	Raketový motor, tekuté palivo, tryska
Keywords:	Rocket engine, liquid propellant, nozzle

Anotace:

česky: Cílem této práce je navrhnout, vymodelovat a ověřit numerickými simulacemi malý experimentální nízkoimpulsní raketový motor na tekuté pohonné látky.

anglicky: The goal of this thesis is to design and verify via numerical simulations a small experimental liquid propellants rocket engine.

Acknowledgement

I would like to thank to Mgr. Jaroslav Kousal Ph.D. for his guidance and assistance during my work on this master thesis.

My deepest gratitude is also towards my family, that has supported me not only during my work on this thesis, but throughout my entire life as well, and to my girlfriend, who became the light in the darkness of the pandemic times and kept me motivated to continue.

Last but not least I would like to thank to past and present employees of NASA, ESA, SpaceX and all other space agencies for their incredible work and overwhelming achievements which kept me fascinated about aerospace engineering.

Table of contents

I. Introduction

While the first concept of rockets dates back into the 13th century, when the first gunpowder powered rockets evolved in medieval China, it took hundreds of years, before this unique kind of propulsion reached space. And although it started as a short range military weapon and firework, thanks to the massive development in the space race era this invention turned into a peaceful mean of space exploration and transportation.

Now, at the beginning of the new space era of reusable launchers, private space tourism, deep space exploration and the potential need of the human civilization going interplanetary, the rocket propulsion has a greater importance than ever before.

II. Theory

2.1. Basics

2.1.1. Laws of physics

Rockets as we know them are powered by a propulsion device called “rocket engine” or “rocket motor” (depending on the state of fuel used). These engines can vary in size, performance, the combustion cycle, but all of them share the same principle of operation.

Rockets follow the Newton's Third Law of Motion, which states:

"For every action there is an equal and opposite reaction."

This means, as the rocket engine produces a force (in this case a thrust) in the direction of the nozzle, equal force is applied back at rocket body in opposite direction.

This is achieved by chemical reaction of the fuel and oxidizer (collectively called “propellants”) in the combustion chamber of the engine, where they are mixed and burned at high temperature, forming hot gases which expand rapidly. These gases are then ejected at high velocity through the nozzle, creating thrust and accelerating the engine in opposite direction. *[1]*

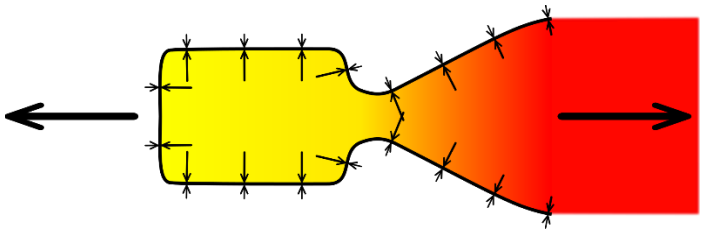

Fig. 1 – force diagram for rocket engine [2]

The acceleration of the rocket follows the Newton's Second Law of Motion, according to which the rate of change of momentum of a rocket is proportional to the applied force - the change in momentum occurs in the direction of the applied force“.

This can be mathematically described as:

$$F = m * \frac{dv}{dt} = m * a \qquad \text{(Eq. 1)}$$

Where:

F = net force applied

m = assumed constant mass of the rocket

dv/dt = change in velocity of the rocket in time

a = acceleration

However, as rockets burn the fuel and therefore are considered to be variable-mass objects, it is necessary to accurately describe their motion. The correct equation for rocket behaviour therefore is:

$$F = m(t) * \frac{dv}{dt} - u * \frac{dm}{dt} \qquad \text{(Eq. 2)}$$

Where:

m(t) = rocket mass variable in time

u = velocity of ejected mass ***relative to the rocket***

dm/dt = ejected mass in time (mass flow rate)

2.1.2. Specific impulse

The specific impulse I_{sp} represents the total impulse per unit weight of the propellant. It is an important figure of merit of the performance of any rocket propulsion system, a concept similar to miles per gallon parameter as applied to automobiles. A higher number indicates better performance. The specific impulse is measured in seconds. *[3]*

2.1.3. Tsiolkovsky equation

The Tsiolkovsky rocket equation, classical rocket equation, or ideal rocket equation is a mathematical equation that describes the motion of vehicles that follow the basic principle of a rocket: a device that can apply acceleration to itself using thrust by

expelling part of its mass with high velocity can thereby move due to the conservation of momentum. *[4]*

This equation relates the delta-v (the maximum available change of velocity of the rocket) to the effective exhaust velocity of the rocket engine and the initial and final mass of a rocket (as the fuel is burnt and the mass therefore decreases).

$$\Delta \mathrm{v} = \mathrm{v}_e * \ln\left(\frac{m_{initial}}{m_{final}}\right) \qquad \text{(Eq. 3)}$$

2.2. Types of propulsion

Rockets are powered by various types of engines. Each type has its own advantages and disadvantages:

- **Solid propellant propulsion -** the propellant is burned in a solid state. Solid-propellant motors are relatively cheap to build, maintain and operate. They are usually highly reliable and produce significant amount of thrust. The disadvantage is, that once the fuel is ignited the motor cannot be shut down by any mean and it is not possible to control the amount of thrust. Solid propellant motors tend to have worse specific impulse than standard liquid propellant engines.
  Solid propellant motors are mostly used as first-stage boosters to improve the rocket performance at the lift off and early in the flight. However for example ESA's rocket Vega utilizes 3 solid fuel stages and only use liquid propulsion at the fourth uppermost stage for orbital insertions.

- **Liquid propellant propulsion –** in this kind of propulsion the liquid fuel and oxidizer are stored in separate tanks. These two ingredients are then fed into the combustion chamber either via pressure (pressure-fed engines) or via pumps, where they burn in a specific mixture ratio. These engines are quite complex, but the advantage is that the thrust can be reduced to some extent mid-flight and they can be shut down safely at any time and in some cases even reignited if designed to do so. They run on a wide range of fuels, such as Hydrogen, Kerosene (RP-1), Hydrogen, or Hydrazine. Although expensive and complex, liquid propellant engines are the most common type of spacecraft propulsion devices.

- **Hybrid propulsion –** in this case the solid propellant is stored in the combustion chamber, to which a second propellant in the form of liquid or gas (most often the oxidizer) is injected to initiate the combustion. Hybrid rocket engines avoid the most common disadvantages of solid and liquid rocket motors/engines (propellant handling and mechanical complexity). However they have their own disadvantages, for example the non-optimal mixing of propellants in different states of matter. Another disadvantage is, that some part of the solid fuel has to be left unburned, to avoid its disintegration and jamming the nozzle, potentially leading to a complete failure of the engine.

- **Monopropellant propulsion –** these engines use a single chemical as the propellant, which is decomposed by a catalyst. The most common monopropellant is hydrazine, which is extremely toxic. These monopropellant engines are very simple in the concept, but their specific impulse is significantly worse than in case of liquid engines.

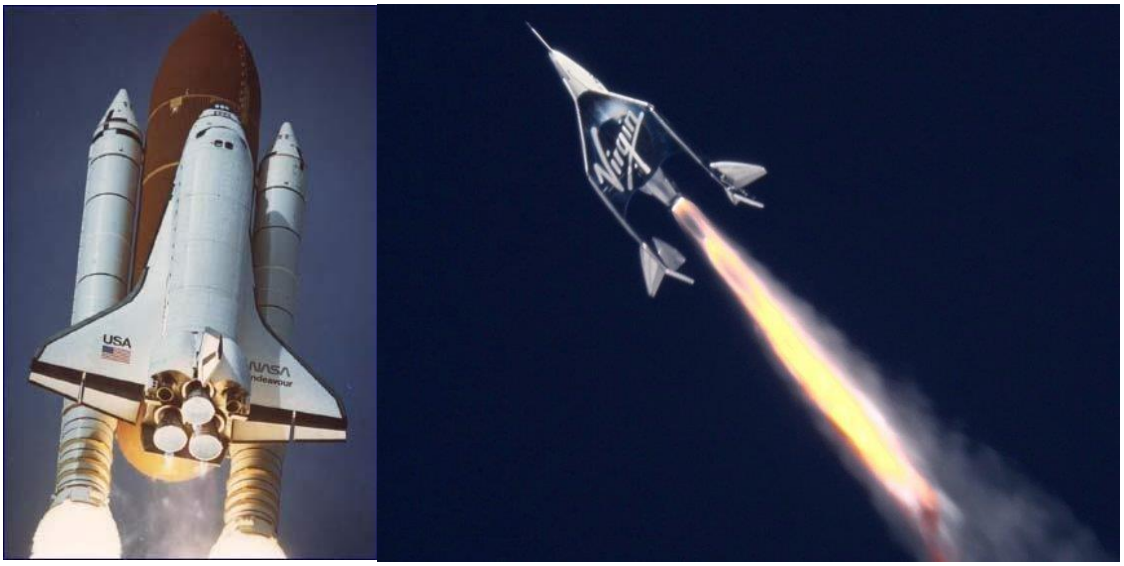

Fig. 2 - Space Shuttle Endeavour with 2 solid-propellant boosters and 3 RS-25 liquid hydrogen/oxygen engines [5] (On the left); Virgin Galactic's SpaceShipTwo with single hydroxyl-terminated polybutadiene (HTPB) hybrid rocket engine [6] (On the right)

2.3. Nozzle

With the exception for highly experimental rocket projects (at this time, as far as I know, only the ARCAspace corporation attempts to utilize an aerospike nozzle), all rocket engines use a **de Laval nozzle** (also known as **convergent-divergent nozzle**) – this nozzle consist of a tube with its cross-section area decreasing in the first half and then expanding again. The hot, pressurized gas is accelerated through the throat of the nozzle to a higher supersonic speeds by converting the heat energy of the flow into kinetic energy. As the gas travels through the nozzle, the pressure and temperature both decrease, while the relative speed increases.

In the ideal case of maximal propulsion efficiency, the gas pressure at the exit of the nozzle is equal to the ambient pressure of the atmosphere.

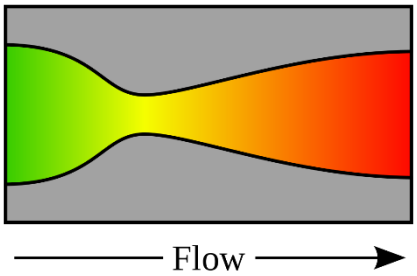

Fig. 3 - Example of de Laval nozzle, the flow velocity increasing from green to red in the direction of flow [7]

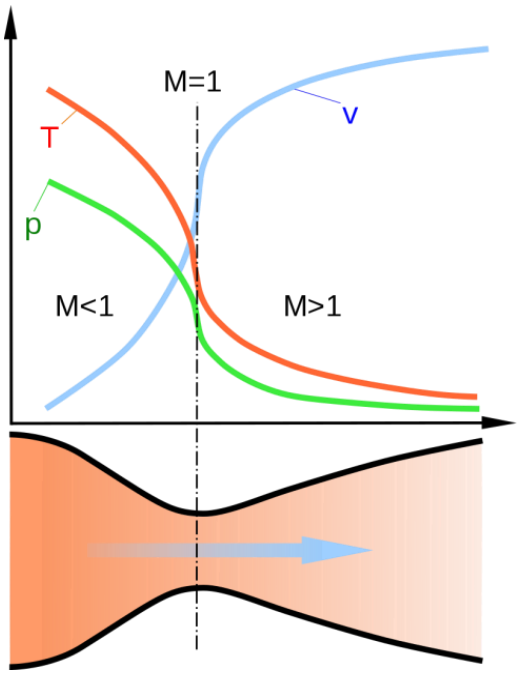

Fig. 4 - Diagram of a De Laval nozzle [8]
where:
v = flow velocity
T = temperature
p = pressure

The linear velocity of the exhaust gases at the nozzle exit area can be calculated with this equation:

$$v_e = \sqrt{\frac{TR}{M} \cdot \frac{2\gamma}{\gamma - 1} \cdot \left[1 - \left(\frac{p_e}{p}\right)^{\frac{\gamma-1}{\gamma}}\right]} \qquad \text{(Eq. 4)}$$

Where:

v_e *= exhaust velocity at the nozzle exit*

T = absolute temperature of inlet gas

R = universal gas law constant (8314.5 J/kmol·K)

M = molecular mass of the gas

γ = c_p/c_v *= isentropic expansion factor*

c_p *= specific heat of the gas at constant pressure*

c_v *= specific heat of the gas at constant volume*

p_e *= absolute pressure of the exhaust gas at the exit of the nozzle p = absolute pressure of the inlet gas*

The nozzle efficiency is significantly affected by its shape and size. Bell-shaped nozzles are the most common nozzles used for rockets, as they can be shorter and lighter compared to simple cone-shaped ones. They are slightly more efficient as well by approx. 1%. They are more complex and therefore more difficult to manufacture.

Apart from these two examples, there are other advanced nozzle designs (such as already-mentioned aerospike nozzle, or stepped (dual-bell) nozzle). These nozzles bring new advantages and challenges with them, but aren't widely used in the space industry.

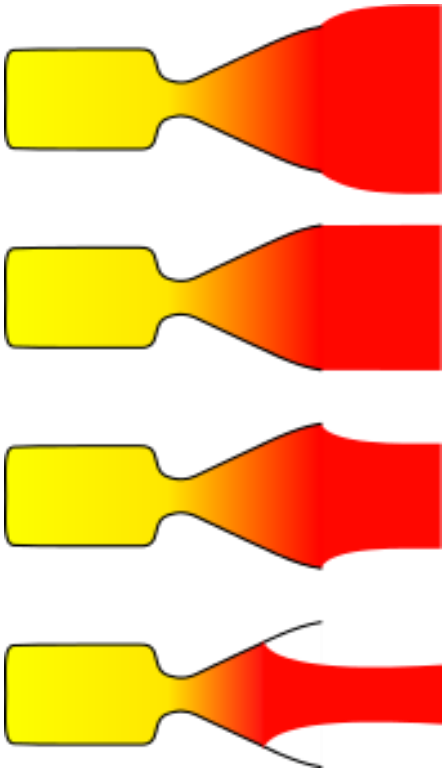

- **under-expanded nozzle** (exit pressure greater than the ambient pressure)
- **perfectly expanded nozzle** (exit pressure equals the ambient pressure)
- **over-expanded nozzle** (exit pressure is smaller than the ambient pressure)
- **grossly over-expanded nozzle** (same problem as overexpanded, but with a shock wave forming inside the divergent nozzle section)

Fig. 5 - Different scenarios of nozzle expansion [9]

2.4. Deeper understanding of liquid-propellant engines

2.4.1. History of liquid propellant engines

The idea of liquid rocket as understood in the modern context first appears in the book The Exploration of Cosmic Space by Means of Reaction Devices, by the Russian school teacher Konstantin Tsiolkovsky. This seminal treatise on astronautics was published in May 1903, but was not distributed outside Russia until years later. *[10]*

The first *flight* of a liquid-propellant rocket took place on March 16, 1926 at Auburn, Massachusetts, when American professor Dr. Robert H. Goddard launched a vehicle using liquid oxygen and gasoline as propellants. The rocket, which was dubbed "Nell", rose just 41 feet during a 2.5-second flight that ended in a cabbage field, but it was an important demonstration that rockets utilizing liquid propulsion were possible. *[10]*

Fig. 6 – Robert H. Goddard with the first working liquid rocket experiment [11]

The next important development followed in Germany, where engineers and scientists tested the possibilities of liquid propellant engines in the early 1930s in a field near Berlin. One of these scientists, Wernher von Braun, later became the head of the army research station that designed the infamous V-2 rocket weapon for the Nazis. *[12]*

Fig. 7 - Von Braun's V-2 rocket [13]

After World War II the American government and military finally seriously considered liquid-propellant rockets as weapons and began to fund work on them. The Soviet Union did likewise, and thus began the Space Race. Von Braun joined the American side and became the chief architect of the Saturn V super heavy-lift launch vehicle that propelled the Apollo spacecraft to the Moon. [12]

2.4.2. Fuels

The liquid propellant rocket engines usually use the bi-propellant system – the fuel and the oxidizer are stored in separate tanks and are mixed in the chamber, where there are combusted. There are various types of fuel used, most common combinations can be found in the following table:

Liquid propellants in various flight vehicles			
rocket		**oxidizer**	**fuel**
German V-2		liquid oxygen	ethyl alcohol–water (75%–25%)
Atlas ICBM		liquid oxygen	RP-1 (kerosene)
Delta	first stage	liquid oxygen	RP-1 (kerosene)
	second stage	nitrogen tetroxide	hydrazine-UDMH* (50%–50%)
Saturn	first stage	liquid oxygen	RP-1 (kerosene)
	second stage	liquid oxygen	liquid hydrogen
	third stage	liquid oxygen	liquid hydrogen
Apollo lunar module		nitrogen tetroxide	hydrazine-UDMH* (50%–50%)
space shuttle	main engines	liquid oxygen	liquid hydrogen
	orbital maneuvering system	nitrogen tetroxide	monomethyl hydrazine
Ariane 4, first stage		nitrogen tetroxide	UDMH*
Energia, first stage	core	liquid oxygen	liquid hydrogen
	cluster	liquid oxygen	kerosene

Tab. 1 – Liquid propellants in various flight vehicles [14]

2.4.3. Engine cycles

For liquid propellant rockets, four different ways of powering the injection of the propellant into the chamber are in common use.

Fuel and oxidizer must be pumped into the combustion chamber against the pressure of the hot gasses being burned, and engine power is limited by the rate at which propellant can be pumped into the combustion chamber. For atmospheric or launcher use, high pressure, and thus high power, engine cycles are desirable to minimize gravity drag. For orbital use, lower power cycles are usually fine. [10]

Pressure-fed cycle

The propellants are forced in from pressurised (relatively heavy) tanks. The heavy tanks mean that a relatively low pressure is optimal, limiting engine power, but all the fuel is burned, allowing high efficiency. The pressurant used is frequently helium due to its lack of reactivity and low density. [10]

Gas-generator cycle

A small percentage of the propellants are burnt in a preburner to power a turbopump and then exhausted through a separate nozzle, or low down on the main one. This results in a reduction in efficiency since the exhaust contributes little or no thrust, but the pump turbines can be very large, allowing for high power engines. Examples: Saturn V's F-1 and J-2, Falcon 9's Merlin. [10]

Expander cycle

Cryogenic fuel (hydrogen, or methane) is used to cool the walls of the combustion chamber and nozzle. Absorbed heat vaporizes and expands the fuel which is then used to drive the turbopumps before it enters the combustion chamber, allowing for high efficiency, or is bled overboard, allowing for higher power turbopumps. Examples: RL10 for Atlas V and Delta IV second stages (closed cycle). [10]

Staged combustion cycle

A fuel- or oxidizer-rich mixture burns in a preburner, then drives turbopumps, and this high-pressure exhaust is fed directly into the main chamber where the remainder of the fuel or oxidizer undergoes combustion, permitting very high pressures and efficiency. [10]

Full-flow staged combustion cycle

Fuel- and oxidizer-rich mixtures are burned in separate preburners and driving the turbopumps, then both high-pressure exhausts, one oxygen rich and the other fuel rich, are fed directly into the main chamber where they combine and combust, permitting very high pressures and incredible efficiency. Example: SpaceX Raptor. [10]

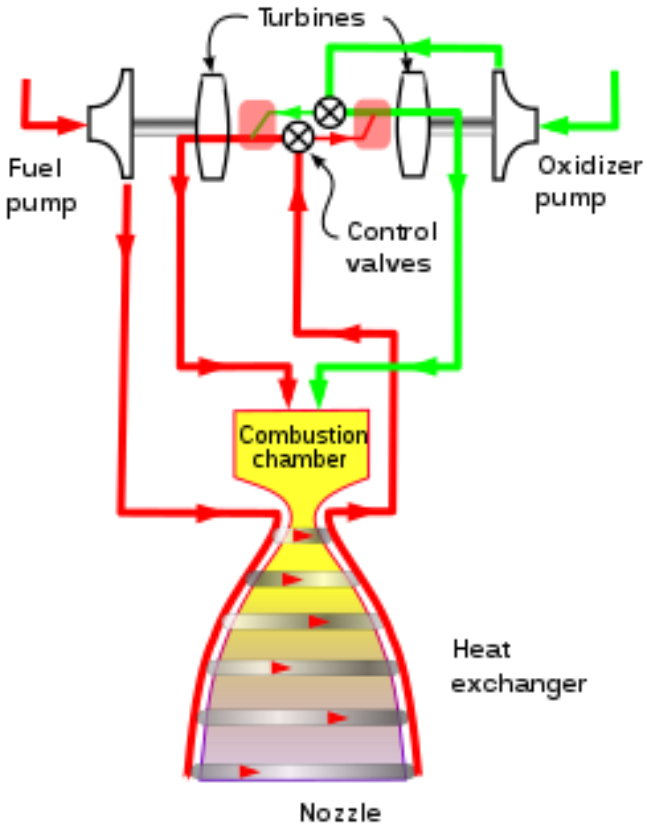

Fig. 8 – Diagram of a full flow staged rocket cycle [15]

	Cycle type			
	Gas generator	**Expander cycle**	**Staged-combustion**	**Pressure-fed**
Advantages	Simple; low dry mass; allows for high power turbopumps for high thrust	High specific impulse; fairly low complexity	High specific impulse; high combustion chamber pressures allowing for high thrust	Simple; no turbopumps; low dry mass; high specific impulse
Disadvantages	Lower specific impulse	Must use cryogenic fuel; heat transfer to the fuel limits available power to the turbine and thus engine thrust	Greatly increased complexity &, therefore, mass (more-so for full-flow)	Tank pressure limits combustion chamber pressure and thrust; heavy tanks and associated pressurization hardware

Tab. 2 - Tradeoff comparison among popular engine cycles [10]

III. Experimental part

3.1. Foreword and introduction

Before we fully move to the experimental part of the thesis, I'd like mention few things.

First of all, this project was supposed to be much more extensive. Just like my Bachelor thesis, which I am really proud of, the goal was to fully develop a working rocket engine, including manufacturing and at least one static test, proving the design works as intended. Unfortunately, soon after I started to work on this project back in 2020, the COVID-19 disease did spread to the world and paralyzed the society. With university's doors closed, it became next to impossible to manufacture, build and test the engine on the academic ground. As a result of this, the physical test phase was replaced with less interesting, but hopefully equally valuable form of performance verification – numerical simulations.

For those not familiar with my Bachelor project, I made a short review of the stuff I worked on two years ago:

3.1.1. Bachelor thesis review

My goal was to design a custom, fully-working small experimental solid-propellant rocket motor with thrust of roughly 100 N and total impulse of 100 to 160 Ns. With the help of Richard Nakka's Experimental Rocketry Web Site I obtained all necessary values needed for designing the motor. In the Autodesk Inventor 2017 I created a 3D assembly model and generated all necessary documentation for manufacturing.

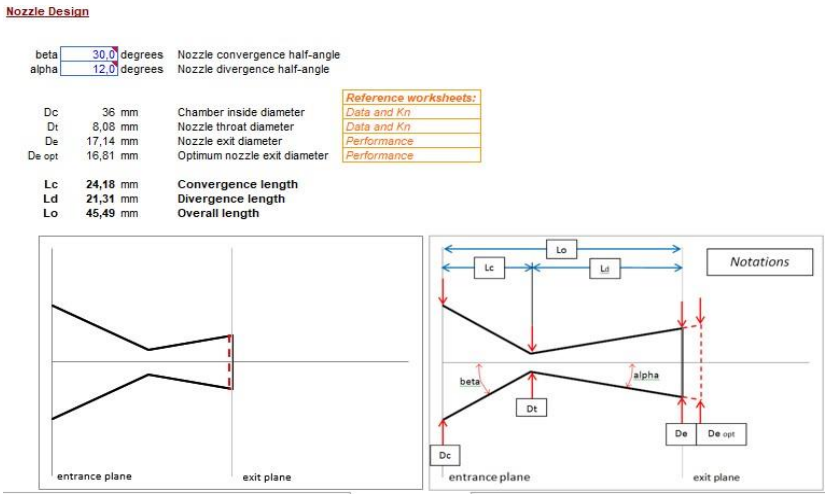

Fig. 9 - Proposed nozzle geometry

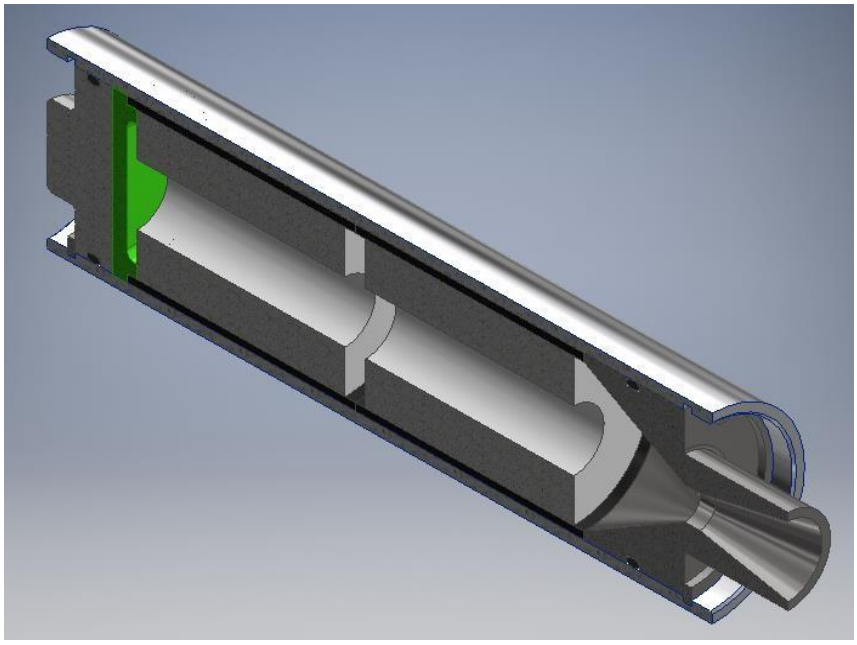

Fig. 10 - Cut through the 3D assembly model

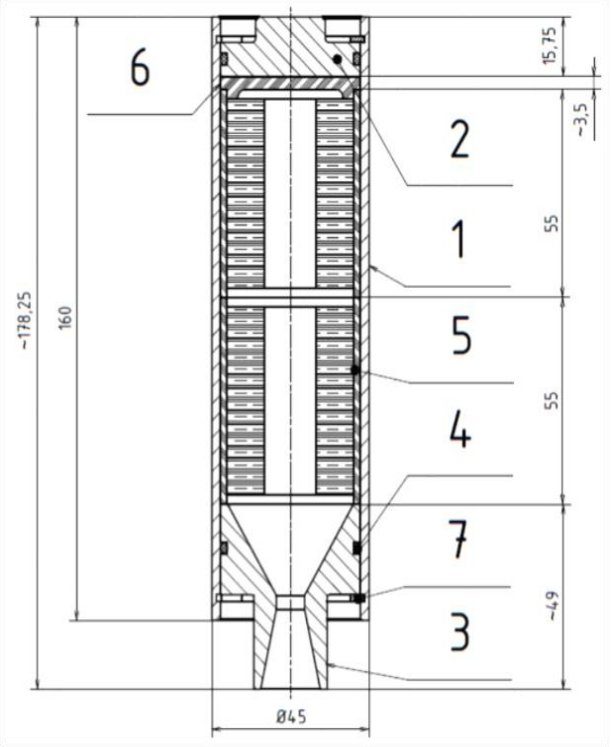

Fig. 11 - Assembly documentation

The usual fuel mixture consisting of 65% of KNO_3 and 35% of Sorbitol was used for this purpose, however I tested several different compositions of the propellant to achieve highest performance possible. It turned out, that the mixture of finely milled KNO_3 with melted Sorbitol, casted into the PVC inhibitor was the best option.

Fig. 12 - Propellant tests

Fig. 13 - Finished BATES propellant grains

Then on 17th July 2019 the experimental motor was successfully fired at the ground of Czech Technical University in Prague. The test was very smooth and data were successfully recovered.

Fig. 14 - Measuring stand with attached motor

Fig. 15 - Views from two testing cameras

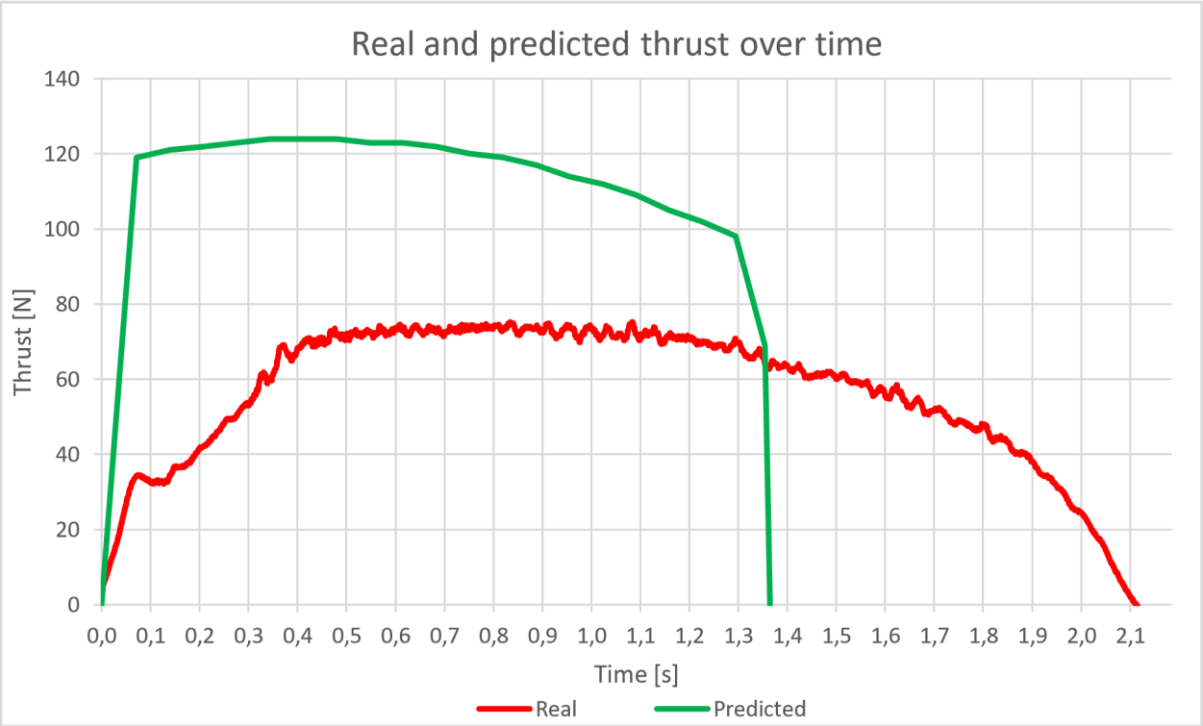

Fig. 16 - Calculated (green line) and measured (red line) results

The peak thrust was lower than expected (75 N instead of 124 N) but the burn time was significantly longer (2,1 s instead of 1,35 s). It turned out the propellant mixture was still very different from the mathematical model and burned slower than expected. This resulted in lower chamber pressure and thus lower thrust, however the burn time was much longer, making the total impulse somewhat comparable (120 Ns instead of 158 Ns).

This motor was fired once more later in 2020, as it was selected to be the critical component of proposed team project rocket. This modified test delivered the peak thrust of 240 N and total impulse of 155 Ns. Unfortunately due to ongoing COVID-19 restrictions this team project didn't continue beyond this point and was eventually cancelled.

3.2. Development

The development started with the research of available materials. While it was clear, that the design will not leave the virtual world (at least within the extent of this thesis) the aim was still to design a relatively cheap liquid-fuelled rocket engine, that could be used as an educational equipment on the Czech Technical University in the future.

While I had some practical experience with development of experimental rocket motors from my bachelor thesis, the development of liquid-fuelled engine was a whole new level to deal with. Thankfully there were many great sources of knowledge on the internet, that helped me to orientate in this new area of aerospace science.

The primary source to my work was a book „How to design, build and test small liquid-fuel rocket engines“ written in 1967 by L. J. Kryczki. While the majority of the mathematical background of this development comes directly from well-proven equations in this book, the mechanical design itself reflects many own thoughts and ideas and should be up to 21st century’s engineering standards.

3.2.1. The design calculations

3.2.1.1. Propellant selection

The very first in the development of own experimental rocket engine is to select an appropriate propellant and oxidizer mixture and working conditions. The table below contains some basic, experimentally measured data, that would help with this decision.

Propellant Combination Oxidizer/Fuel	Combustion Pressure, psi	Mixture Ratio	Flame Temp °F	Isp, sec
Liquid oxygen & gasoline	300	2.5	5470	242
Gaseous oxygen & gasoline	300	2.5	5742	261
Gaseous oxygen & gasoline	500	2.5	5862	279
Liquid oxygen & JP-4 (jet fuel)	500	2.2	5880	255
Liquid oxygen & methyl alcohol	300	1.25	5180	238
Gaseous oxygen & methyl alcohol	300	1.2	5220	248
Liquid oxygen & hydrogen	500	3.5	4500	363
Red fuming nitric acid & JP-4	500	4.1	5150	238

Note: expansion to 14.7 psi

Tab. 3 – Calculated performance of some liquid propellants [16]

For this engine the primary goal is to use widely available and easily accessible sources of energy. For this reason, I went with the mixture of gaseous oxygen and liquid methyl alcohol. The table above suggest the mixture ratio of 1,2 and working pressure of 300 psi. This is great, as this pressure is very close to 2 MPa, which was the value I used for the rocket motor in my Bachelor thesis, therefore the environment I had a practical experience with.

The following diagrams will help with determination of some other working aspects of this engine, specifically the temperature and specific impulse of the engine.

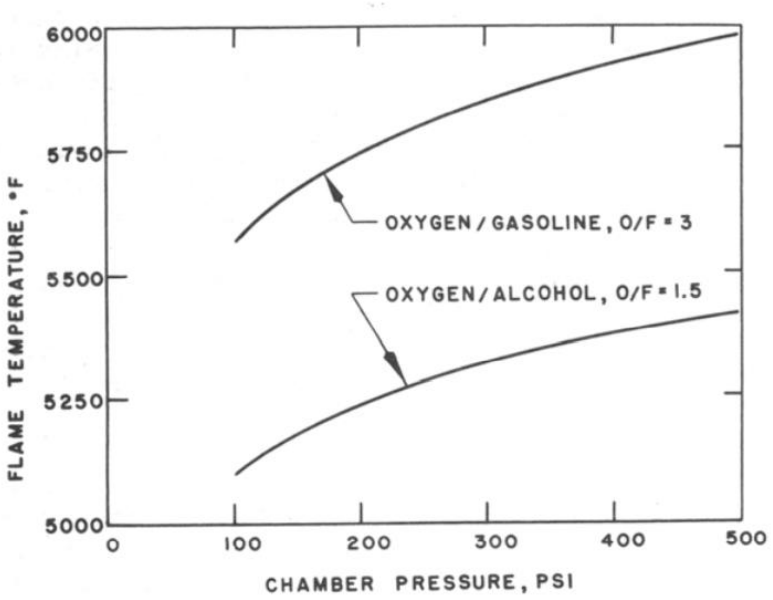

Fig. 17 – Flame temperature vs. the chamber pressure [17]

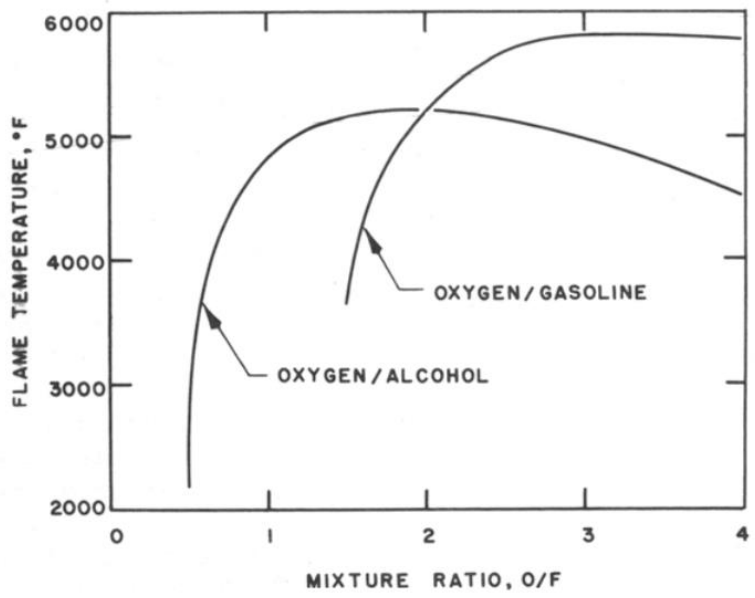

Fig. 18 – Flame temperature vs. the mixture ratio [18]

From the diagram above we can read, that with the oxidizer/fuel mixture ratio of 1,2 we can expect the temperature of something slightly above 5000 °F. During the time I was performing the calculation, I ended up with a value of 5300 °F ≈ 2926,66 °C.

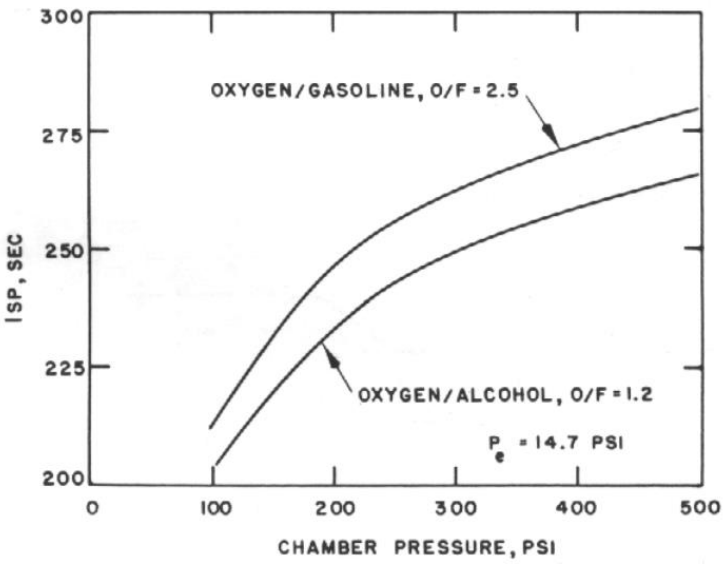

Fig. 19 – Performance of hydrocarbon fuels with gaseous oxygen [19]

As for the expected specific impulse of the engine, the diagram above suggest, that at the working pressure of 300 psi (2,06 MPa), the I_{sp} should be around 250 seconds.

Using all known values, the flow rate can be calculated:

$$W = \frac{F}{I_{sp}} = \frac{100N}{250s} = 0{,}4\ N/s => W_t = 40{,}8\ g/s \quad \text{(Eq. 5)}$$

$$W_f = \frac{W}{r+1} = \frac{40{,}8}{1{,}2+1} = 18{,}55\ g/s \quad \text{(Eq. 6)}$$

$$W_o = \frac{W * r}{r+1} = \frac{40{,}8 * 1{,}2}{1{,}2+1} = 22{,}25\ g/s \quad \text{(Eq. 7)}$$

The mass of fuel and oxidizer necessary for delivering the thrust of 100 N is 40,8 g/s. With the mixture ratio of 1,2 it makes 18,55 g/s of fuel and 22,25 g/s of oxidizer.

3.2.1.2. Nozzle throat temperature

Next step was to determine the hot gas temperature at nozzle throat. This temperature is lower than the combustion chamber temperature, due to the loss of thermal energy as the gas accelerates to the local speed of sound. Therefore:

$$T_t = T_c * \left[\frac{1}{1+\frac{\gamma-1}{2}}\right] = 2926{,}66 * \left[\frac{1}{1+\frac{1{,}2-1}{2}}\right] = 2660{,}6\ °C = 2933{,}75\ K \qquad \text{(Eq. 8)}$$

The nozzle throat temperature is 2933,75 K.

3.2.1.3. Nozzle throat pressure

The pressure at the nozzle throat is determined by following equation:

$$P_t = P_c * \left[1+\frac{\gamma-1}{2}\right]^{-\frac{\gamma}{\gamma-1}} = 2068427 * \left[1+\frac{1{,}2-1}{2}\right]^{-\frac{1{,}2}{1{,}2-1}} = 1\ 167\ 573{,}12\ Pa \qquad \text{(Eq. 9)}$$

Just like the temperature, the pressure drops as well due to the gas accelerating to the local speed of sound. In this case, $P_t \cong$ 1,17 MPa.

3.2.1.4. Nozzle throat area

From all values obtained the nozzle throat area was calculated with following equation:

$$A_t = \left(\frac{W_t}{P_t}\right) * \sqrt{\frac{R * T_t}{\gamma * g}} = \left(\frac{0{,}0408}{1\ 167\ 573{,}12}\right) * \sqrt{\frac{8\ 314{,}4626 * 2\ 933{,}75}{1{,}2 * 9{,}81}} = 5{,}03 * 10^{-5}\ m^2 \qquad \text{(Eq. 10)}$$

3.2.1.5. Nozzle throat diameter

From the circular area it is more than simple to calculate the diameter:

$$D_t = \sqrt{\frac{4 * A_t}{\pi}} = \sqrt{\frac{4 * 5{,}03 * 10^{-5}}{\pi}} = 0{,}008\ m \qquad \text{(Eq. 11)}$$

The nozzle throat diameter is 8 mm.

For comparison, the solid-fuel rocket motor from my Bachelor thesis with very similar performance characteristics (max. thrust of 120 N) had D_t = 8,08 mm.

3.2.1.6. Nozzle exit area

Knowing the optimal ratio between the nozzle exit area and nozzle throat area according to the table below, (for $P_c = 300\,psi$) it was trivial to calculate the nozzle exit area, as well as the nozzle exit diameter.

P_c	M_e	A_e/A_t	T_e/T_c
100	1.95	1.79	0.725
200	2.33	2.74	0.65
300	2.55	3.65	0.606
400	2.73	4.6	0.574
500	2.83	5.28	0.55

Tab. 4 – Nozzle parameters for various chamber pressures [20]

$$A_e = 3{,}65 * A_t = 3{,}65 * 5{,}03 * 10^{-5} = 1{,}836 * 10^{-4}\,m^2 \qquad \text{(Eq. 12)}$$

3.2.1.7. Nozzle exit diameter

$$D_e\sqrt{4 * \frac{A_e}{\pi}} = \sqrt{4 * \frac{1{,}836 * 10^{-4}}{\pi}} = 0{,}015289\,m \qquad \text{(Eq. 13)}$$

The nozzle exit diameter is 15,3 mm. I however like overexpanded nozzles and subsequent Mach diamonds, therefore I used the slightly larger diameter of 18 mm instead.

3.2.1.8. Combustion chamber length

Knowing the nozzle geometry, the next step was to determine the chamber length. To calculate this, a parameter describing the chamber volume required for complete combustion is the characteristic chamber length – L* is needed.

The book suggests, that L* of 50 to 100 inches (1,27 m to 2,54 m) is appropriate for this application.
For further calculation I went with L* = 2 m.

$$V_c = L^* * A_t = 2 * 5{,}03 * 10^{-5} = 1{,}006 * 10^{-4}\ m^3 \quad \text{(Eq. 14)}$$

The chamber volume is therefore $1{,}006 * 10^{-4}\ m^3$.

3.2.1.9. Combustion chamber diameter and length

$$V_c = 1{,}1 * A_c * L_c \quad \text{(Eq. 15)}$$

$$D_c = 5 * D_t = 5 * 0{,}008 = 0{,}04\ m \quad \text{(Eq. 16)}$$

$$A_c = \frac{\pi * D_c^2}{4} = \frac{\pi * 0{,}04^2}{4} = 0{,}0012566\ m^2 \quad \text{(Eq. 17)}$$

$$L_c = \frac{V_c}{1{,}1 * A_c} = \frac{1{,}006 * 10^{-4}}{1{,}1 * 0{,}0012566} = 0{,}07278\ m \quad \text{(Eq. 18)}$$

The camber diameter is 40 mm and the minimal chamber length is 72,78 mm. For design and eventual manufacturing purposes I stick with the chamber length of 80 mm.

3.2.1.10. Combustion chamber wall thickness

To determine the minimal chamber wall thickness made of copper, the following equation was needed:

$$S = \frac{P * D}{2 * t_w} \quad \text{(Eq. 19)}$$

$$t_w = \frac{P * D}{2 * S} = \frac{2\,068\,427{,}2 * 0{,}04}{2 * 60\,000\,000} = 0{,}69\ mm \quad \text{(Eq. 20)}$$

The minimal chamber wall thickness is 0,69 mm. However, since this is supposed to be a static, educational equipment, the safety is the number one priority, and therefore

the wall thickness should be appropriately increased, to avoid the event of rapid unscheduled disassembly at academic grounds.

For this reason I selected the wall thickness to be 3 mm.

Stress check verification:

$$\sigma_a = K = \frac{p_1 r_1^2 - p_2 r_2^2}{r_2^2 - r_1^2} = \frac{2\,068\,427{,}2 * 20^2 - 101\,325 * 23^2}{23^2 - 20^2} = 6{,}0036\ N/mm^2 \quad \text{(Eq. 21)}$$

$$\sigma_{red} = \sigma_{t(r1)} - \sigma_{r(r1)} = (2K + \mathrm{p}_1) - (-\mathrm{p}_1) = (2 * 6{,}0036 + 2{,}0684272) - (-2{,}0684272) = 16{,}144\ N/mm^2 \quad \text{(Eq. 22)}$$

$$k = \frac{\sigma_D}{\sigma_{red}} = \frac{60}{16{,}144} = 3{,}717 \quad \text{(Eq. 23)}$$

The safety coefficient is 3,717.

3.2.1.11. Heat transfer rate

To obtain the approximate values of expected heat transfer it was necessary to calculate the total surface area of the chamber wall, including the nozzle section up to the nozzle throat.

$$A_{cyl} = \pi * (D_c + 2 * t_w) * L_c = \pi * (0{,}04 + 2 * 0{,}003) * 0{,}08 = 0{,}011561\ m^2 \quad \text{(Eq. 24)}$$

$$A_{con} = \pi * L * r = \pi * 0{,}025 * 0{,}02 = 0{,}00157\ m^2 \quad \text{(Eq. 25)}$$

$$A = A_{cyl} + A_{con} = 0{,}011561 + 0{,}00157 = 0{,}013131\ m^2 \quad \text{(Eq. 26)}$$

The book suggests, that the heat transfer rate q is roughly $3\ BTu/in^2 s$. This is a terrible unit to work with, so a unit conversion was needed. Therefore:

$$q = 3\frac{BTu}{in^2 * s} = 4\,905{,}75\frac{kJ}{m^2 * s} \quad \text{(Eq. 27)}$$

The total heat transferred can be then calculated:

$$Q = q * A = 4\,905{,}75 * 0{,}013131 = 64{,}417\ kJ/s \quad \text{(Eq. 28)}$$

3.2.1.12. Coolant flow rate

The coolant flow rate (in this case a water) can be calculated, assuming we know the desired temperature rise of the coolant. I went with a conservative value of 40 °C. For the water, that was 20°C in the beginning it makes the absolute temperature at the outlet 60°C.

$$w_w = \frac{Q}{\Delta T} = \frac{64{,}417}{40} = 1{,}61\ l/s \quad \text{(Eq. 29)}$$

The minimal flow rate of the water is 1,61 l/s, assuming the gap between the walls is constant.

3.2.1.13. Coolant velocity

The book suggests, that the minimal coolant velocity in the annual area between the copper chamber wall and outer jacket should be at least 30 ft/s. This is roughly 10 m/s.

$$v_w = \min 30\ ft/s = 9{,}144\ m/s \rightarrow 10\ m/s \quad \text{(Eq. 30)}$$

$$A = \frac{\pi}{4} * (D_2^2 - D_1^2) \quad \text{(Eq. 31)}$$

$$v_w = \frac{w_w}{\rho * A} \quad \text{(Eq. 32)}$$

$$D_2 = \sqrt{\frac{4 * w_w}{v_w * \rho * \pi} + D_1^2} = \sqrt{\frac{4 * 1{,}61}{10 * 1\,000 * \pi} + 0{,}046^2} = 0{,}04818\ m \quad \text{(Eq. 33)}$$

$$\frac{D_2 - D_1}{2} = \frac{0{,}04818 - 0{,}046}{2} = \frac{0{,}00218}{2} = 0{,}00109\ m \rightarrow 1{,}1\ mm \quad \text{(Eq. 34)}$$

The ideal distance between the chamber wall and outer jacket for the water flow is 1,1 mm.

3.2.1.14. Fuel injector

For this small liquid fuel rocket engine, a commercial spray nozzle shall be used. To select an appropriate spray nozzle, it is necessary to know the orifice diameter. The book suggests to usual pressure drop is about 100 psi.

$$w_f = 18{,}55\ g/s \qquad C_d = 0{,}7 \qquad \rho_{ethanol} = 789\ kg/m^3$$

$$\Delta p \approx 100\ psi = 689\,475{,}73\ Pa$$

$$A = \frac{w_f}{C_d * \sqrt{2 * g * \rho * \Delta p}} = \frac{0{,}01855}{0{,}7 * \sqrt{2 * 9{,}81 * 789 * 689\,475{,}73}} = 2{,}565 * 10^{-7} m^2 \quad \text{(Eq. 35)}$$

$$D = \sqrt{\frac{4*A}{\pi}} = \sqrt{\frac{4*2{,}565*10^{-7}}{\pi}} = 5{,}715 * 10^{-4}\ m = 0{,}5715\ mm \quad \text{(Eq. 36)}$$

The important parameter is also the nozzle capacity:

nozzle capacity = volumetric flow rate in (l/min)*10 at 20 bar

$$w_f * 60 * 10 = 0{,}01855 * 60 * 10 = 11{,}1 \quad \text{(Eq. 37)}$$

The injector orifice diameter should be at least 0,57 mm, while the nozzle capacity parameter should be close to 11,1. Knowing the desired flow rate, geometry and nozzle capacity, the B1/4M-SS10 spray nozzle was selected from the Spaying Systems Co. online catalogue.

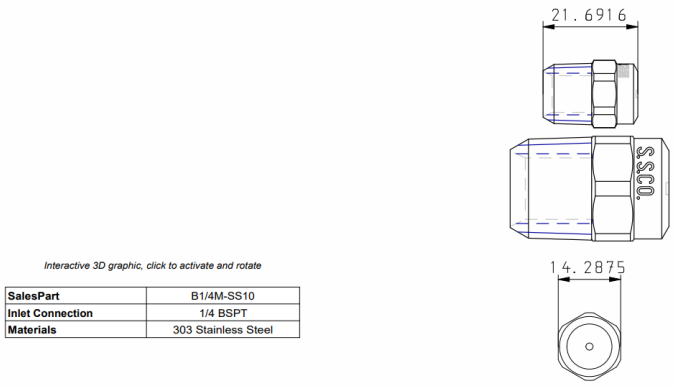

SalesPart	B1/4M-SS10
Inlet Connection	1/4 BSPT
Materials	303 Stainless Steel

Fig. 20 - Spraying nozzle

3.2.1.15. Oxidizer injection

The final step of the preliminary calculation process is to determine the gaseous oxygen intake size and geometry.

$$\rho_2 = \rho_1 * \frac{P_2}{P_1} = 38{,}895 * \frac{2068427}{2757902} = 29{,}171\ kg/m^3 \text{ @300 psi} \quad \text{(Eq. 38)}$$

$$A = \frac{w_o}{\rho * v_o} = \frac{0{,}02225}{29{,}171 * 60} = 1{,}271 * 10^{-5} m^2 \rightarrow 12{,}71\ mm^2 \quad \text{(Eq. 39)}$$

Assuming 8 holes $\rightarrow \frac{12{,}71}{8} = 1{,}589\ mm^2/hole$

$$D = \sqrt{\frac{4 * A}{\pi}} = \sqrt{\frac{4 * 1{,}589}{\pi}} = 1{,}422\ mm \quad \text{(Eq. 40)}$$

Each hole should have the diameter of at least 1,422 mm. For manufacturing purposes I selected the diameter d = 1,5 mm for each of 8 holes.

With all critical parameters obtained, the next step of the development started. For the purpose of 3D modelling of the desired device I used the Autodesk Inventor 2017 CAD application.

The model is pretty simple and straight-forward, however there are few improvements that should increase the durability and improve the heat/coolant distribution.

The major area I paid a lot of attention to was the coolant intake and distribution system. There were multiple options to choose from, as elaborated in following section.

3.2.2. Cooling configurations

Single radial inlet

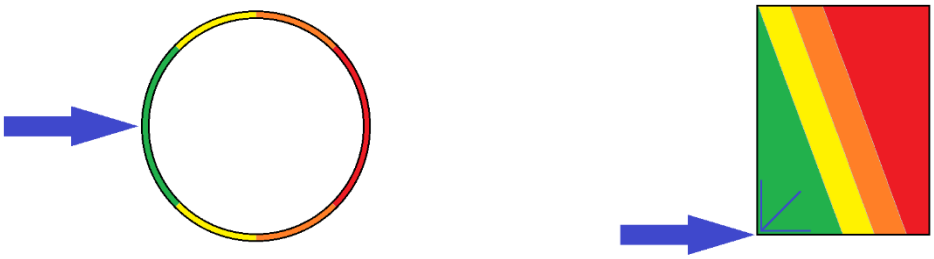

Fig. 21 – Single radial inlet

This is the most basic concept of coolant distribution, also the one proposed in the book. I find this case to be very ineffective and possibly dangerous, due to very uneven temperature gradient across the surface of the chambre wall. This single inlet scenario leads to a hotspot on the opposite side of the chamber.

Dual radial inlet

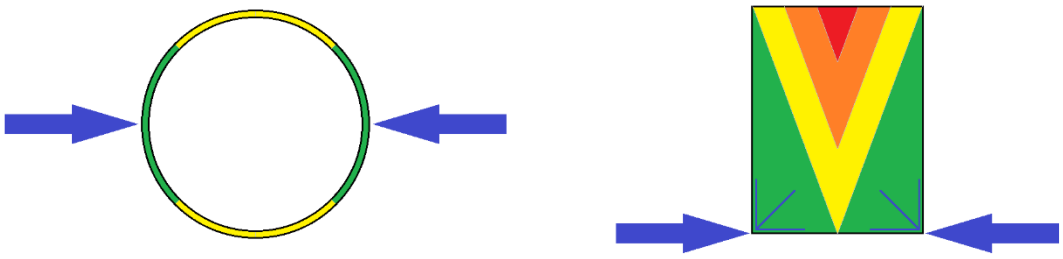

Fig. 22 – Dual radial inlet

The dual radial inlet scenario suggests two coolant inlets on opposing sides of the chamber, instead of just one. This significantly improves the distribution, as coolant is injected on multiple places (could be more than two) and potential hotspots are closer to intakes. There is still a room for improvement, as seen in the final scenario.

Dual tangential inlet

Fig. 23 – Dual tangential inlet

The last scenario is similar to the previous one – two coolant inlets at the bottom of the chamber. However their tangential placement should force the coolant to swirl around whole chamber and should lead to even more uniform distribution with the heat gradient to be close to parallel to the main axis of the engine.

This was the solution I went with in the end. This also meant there had to be two tangential coolant outlets at the top of the chamber to let the water out. I believe other outlet placements would work too, however for the sake of consistency the intake solution was mimicked.

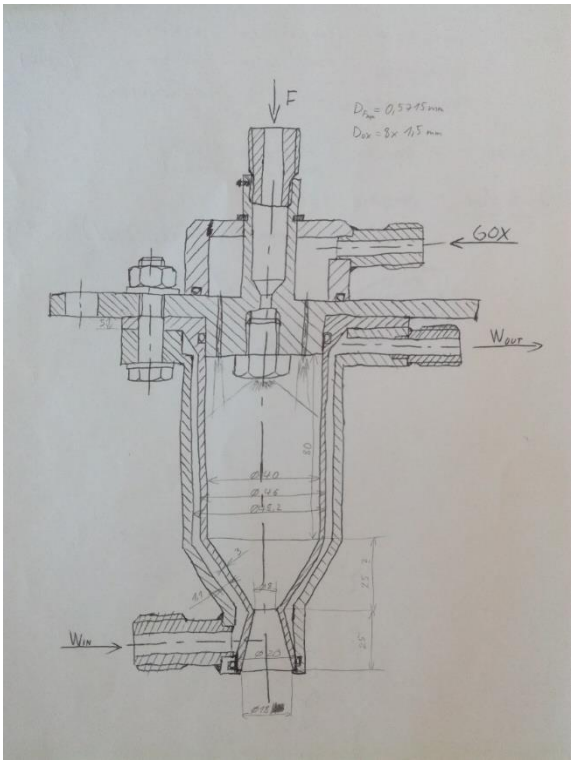

Fig. 24 – Preliminary hand drawing for the CAD model

3.3. The CAD model

For the purpose of 3D CAD modelling I use the Autodesk Inventor 2017 application. Not many comments about the process of modelling, therefore pictures of the finished model follow:

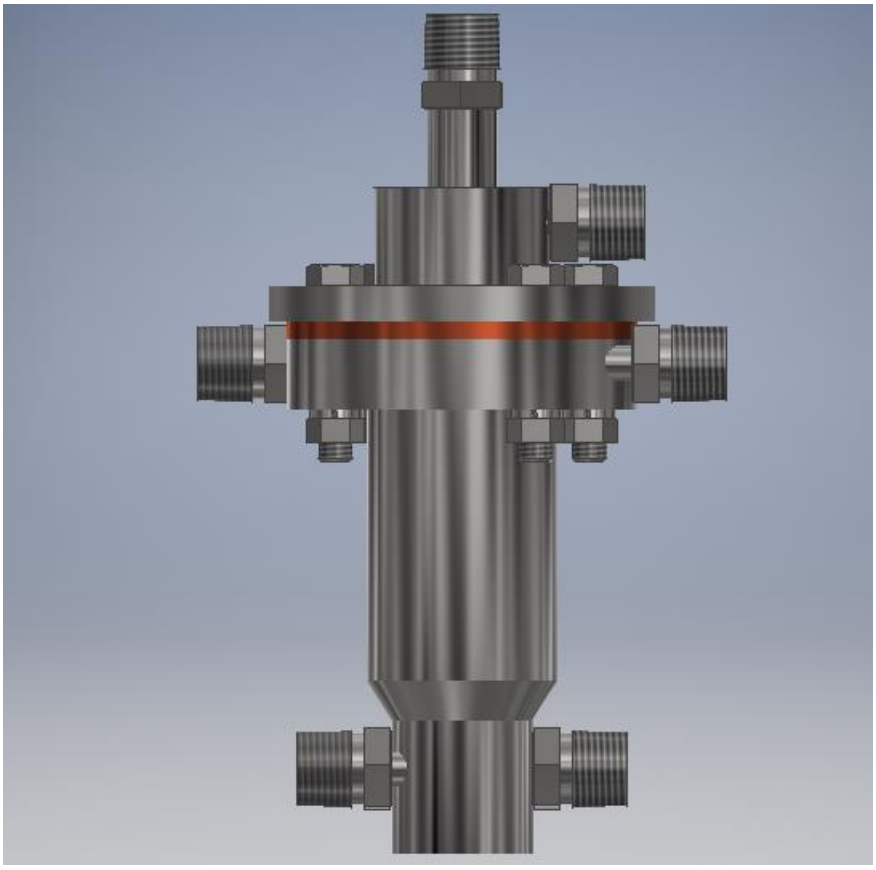

Fig. 25 - Full engine side view

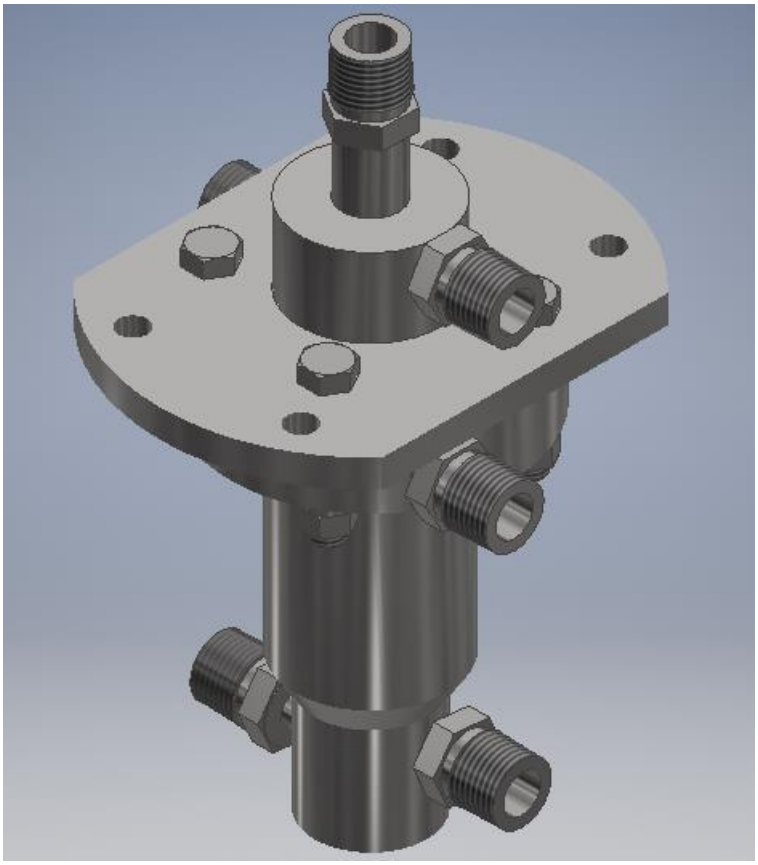

Fig. 26 – Full engine isometric view

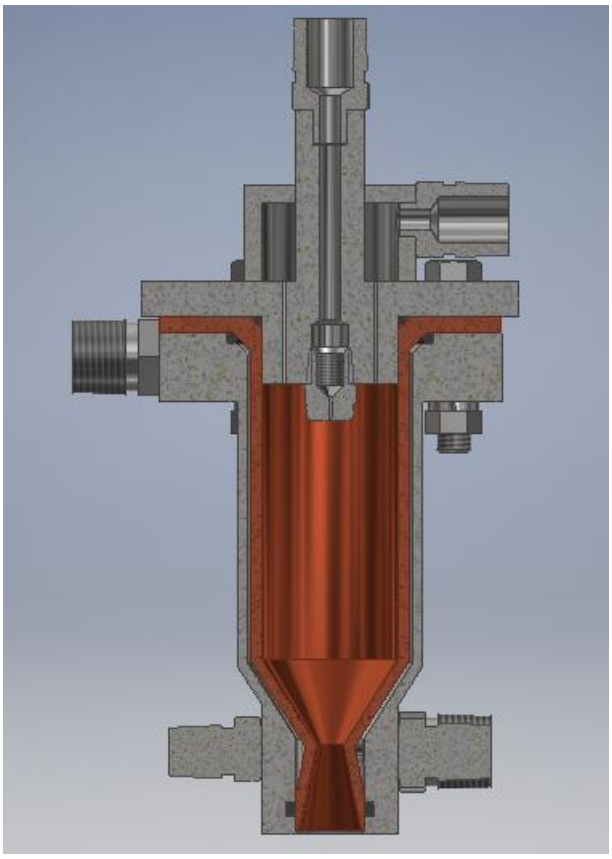

Fig. 27 - Cut through the engine

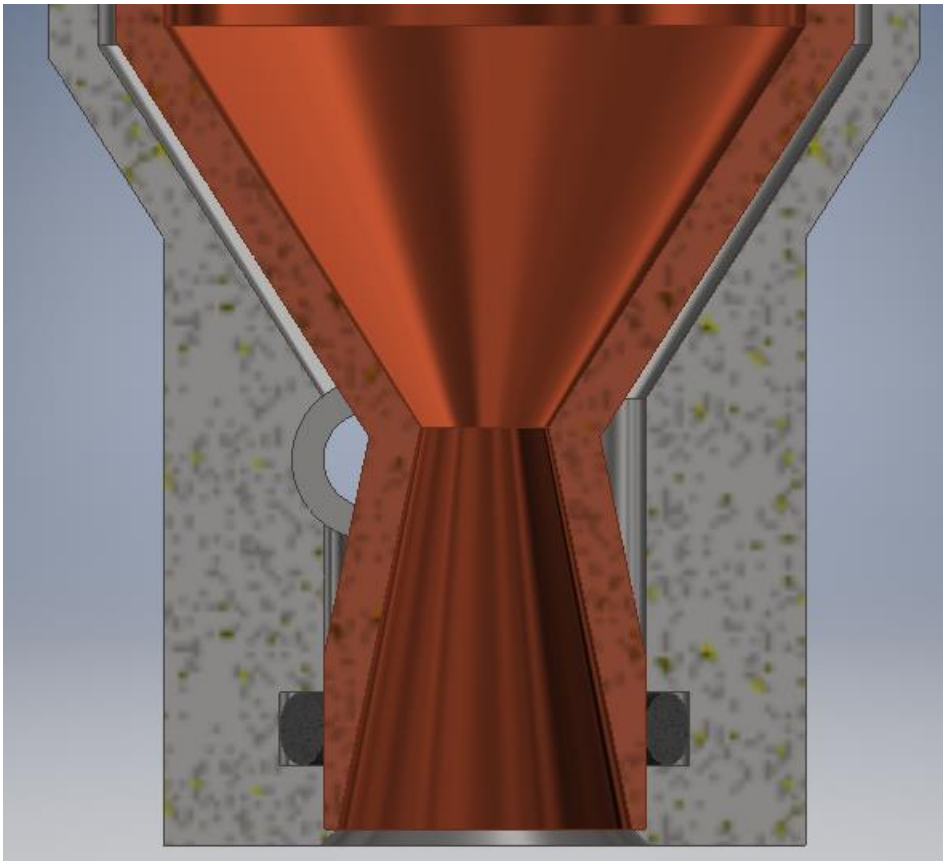

Fig. 28 - Nozzle detail cut with visible offset coolant intake

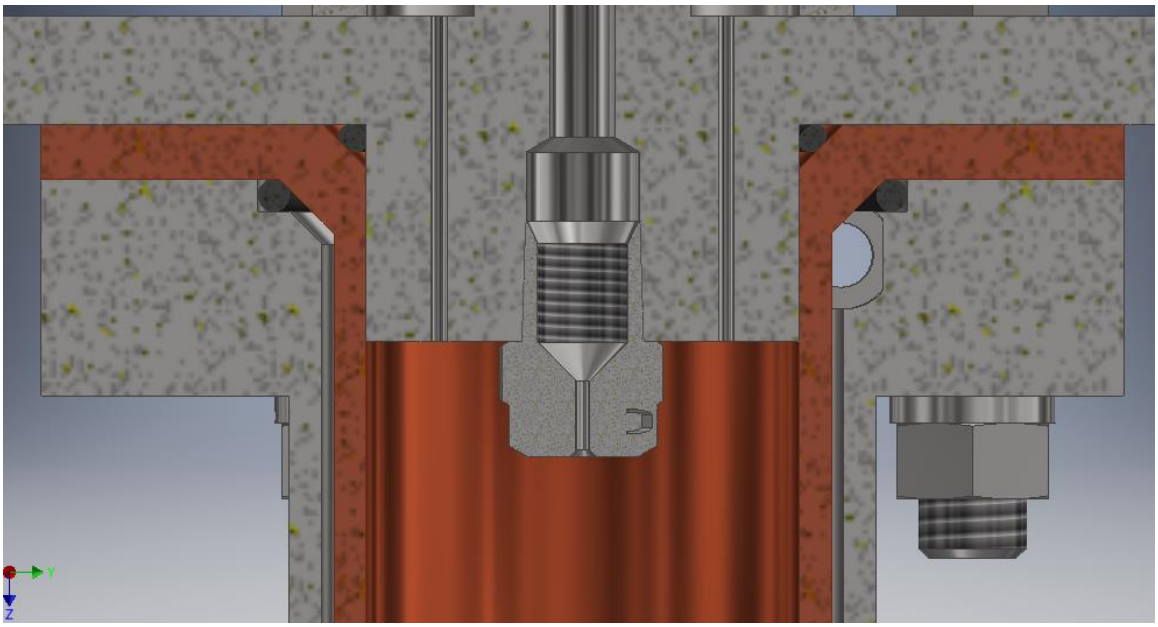

Fig. 29 - Injection detail #1

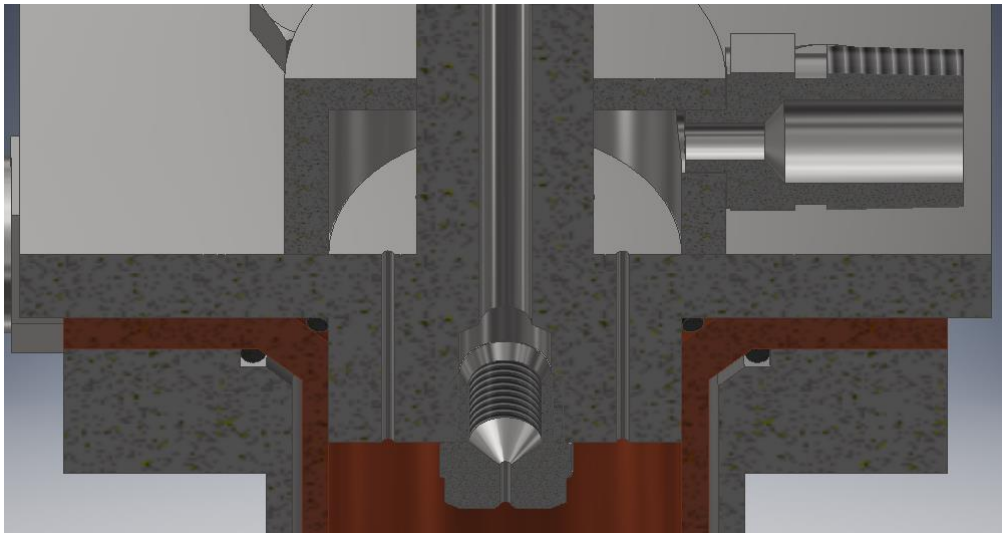

Fig. 30 - Injection detail #2

Due to excessive amount of technical documentation from this model all generated drawings and CAD files are available in the CD attached to the back of this thesis.

3.4. Numerical simulations

As mentioned before, the inability to build the engine within the timeframe of this thesis due to pandemic restrictions forced me to perform a different way of design verification. For this purpose I used the ANSYS 2021 R1 software, where I attempted to create a simplified representation of my design and perform numerical simulations to verify, that the engine works as intended.

There are two individual simulations:

1) The hot gas flow through the engine nozzle and its interaction with outer atmosphere
2) Heat transfer simulation in the cooling mechanism of the engine

3.4.1.1. Exhaust interaction simulation

In this scenario I designed a simplified 2D representation the proposed engine in ANSYS' DesignModeler. This simulation consisted of a big rectangle 1,5 m long and 0,3 m high, representing the space around the engine, and in the corner I cut out the shape of the engine. Then I divided the area inside the engine into smaller sections for easier meshing.

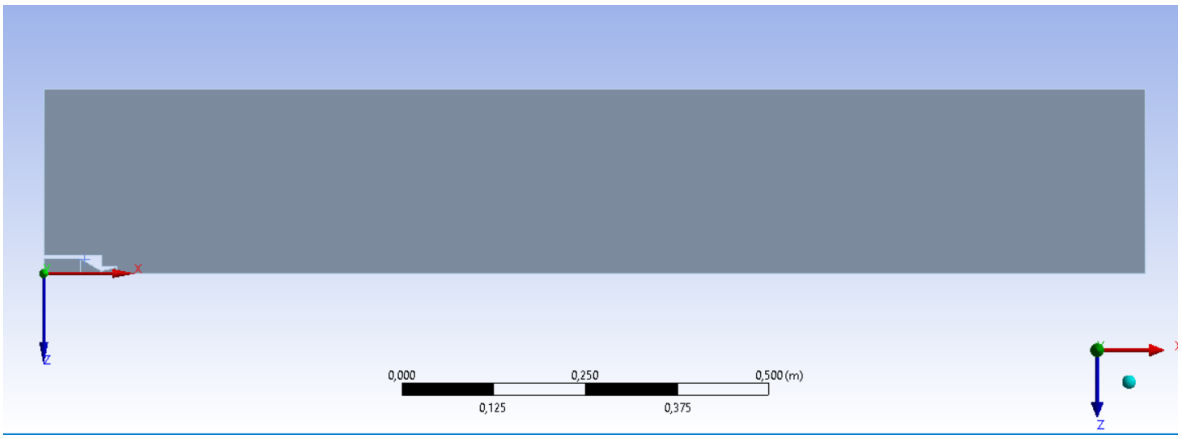

Fig. 31 – Ansys simulation area

As the geometry and conditions are very similar to the solid fuel motor from my Bachelor thesis, I was very optimistic and went with a very dense mesh straight away. For the edge sizing I used the near-wall model approach, decreasing the cell size near the walls as seen in following pictures. For every section I used the pure quadrilateral method of meshing (ensuring there are no triangular shapes anywhere in the simulation).

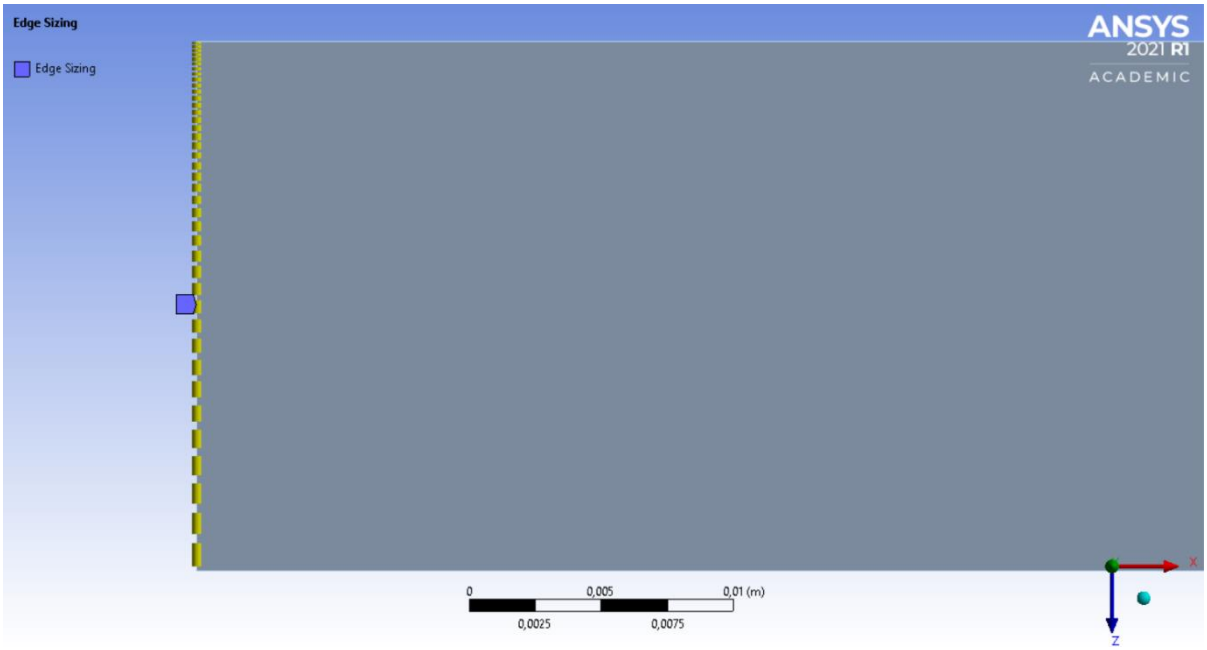

Fig. 32 - Near-wall model approach sizing example

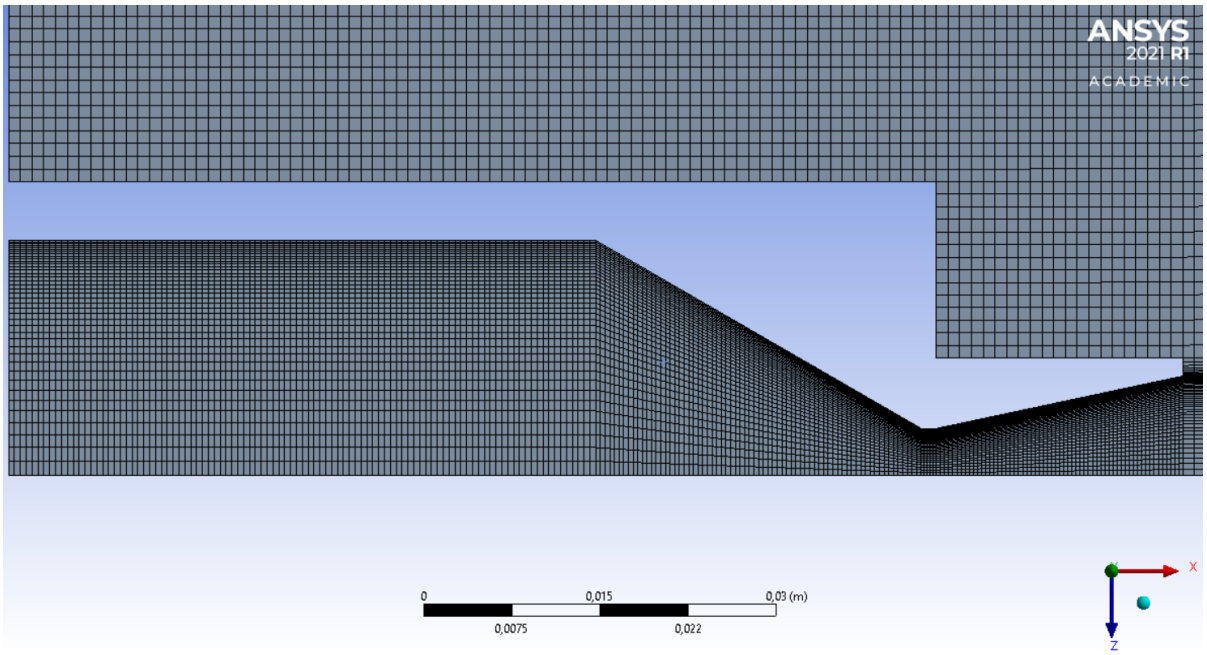

Fig. 33 – Finished mesh

After the meshing was completed, I associated functions to specific edges in Named selections – inlet, outlet, symmetry, walls and the farfield.

Next step was the simulation setup. In the models section, the energy equation was turned on, viscous model used the realizable k-epsilon model with standard wall function of near-wall treatment. No other model was considered in this simulation.

For the hot gasses the Fluent Fluid Material – air was used with the density of ideal gas and Sutherland viscosity.

Then I had to specify the boundary conditions. The inlet was standard pressure inlet with the value of the working pressure equalling 2 068 427 Pa and the temperature of 3200 K. The outlet was treated as a pressure outlet with the conditions of ambient atmosphere – 101,325 Pa and 300 K. The bottom wall was used as the main axis and the symmetry trait was associated. All boundary conditions presenting the engine hardware itself were treated as standard stationary walls with no special properties. Finally, the farfield boundary condition was associated to two remaining walls.

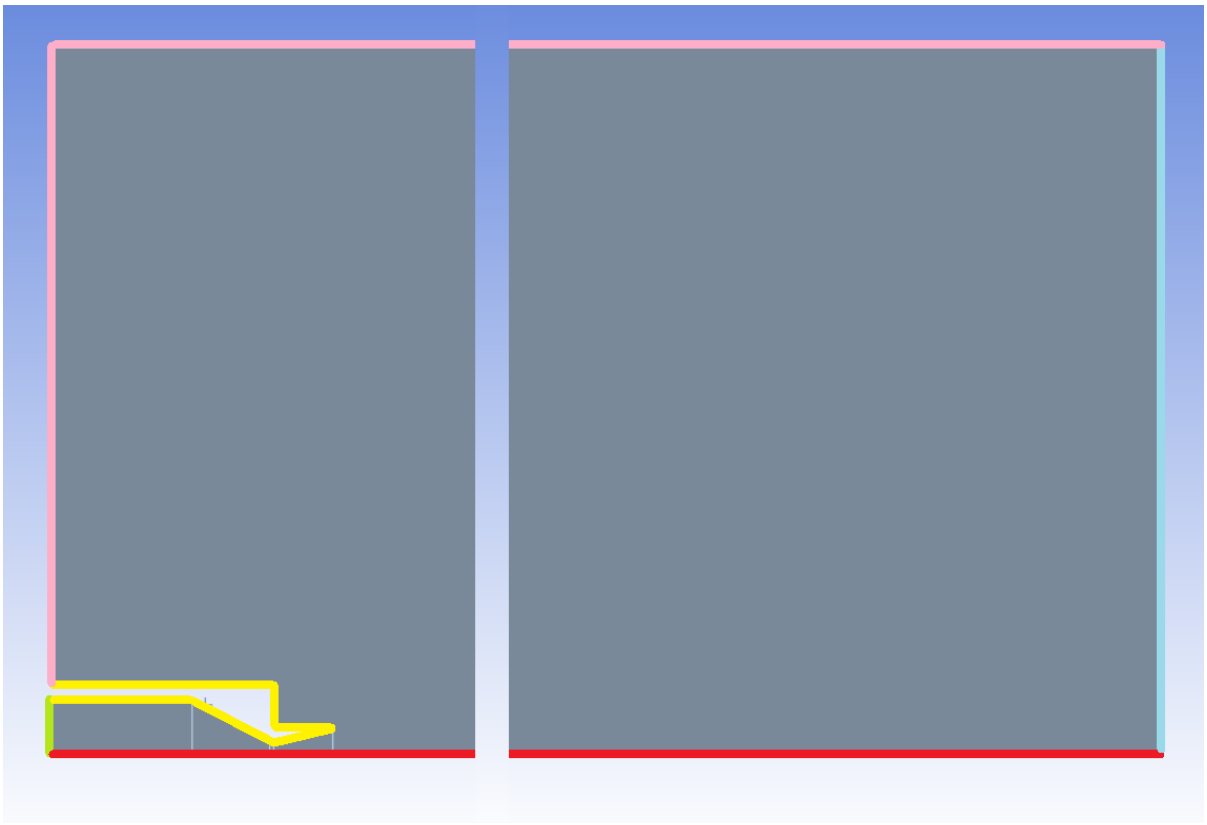

Fig. 34 - Boundary conditions:
Inlet – green; outlet – blue; symmetry – red; walls – yellow; farfield – pink

The solution method had implicit formulation with Roe-FDS flux type. The Gradient used was Least Cell Squares Based and the Flow, the Turbulent Kinetic Energy and the Turbulent Dissipation Rate were all Second Order Upwind.

The standard initialization was performed and the calculation with 5 000 iterations started.

3.4.1.2 Results

The simulation took roughly 3 hours to complete. The expectation was to see a clear exhaust plume with well visible Mach diamonds.

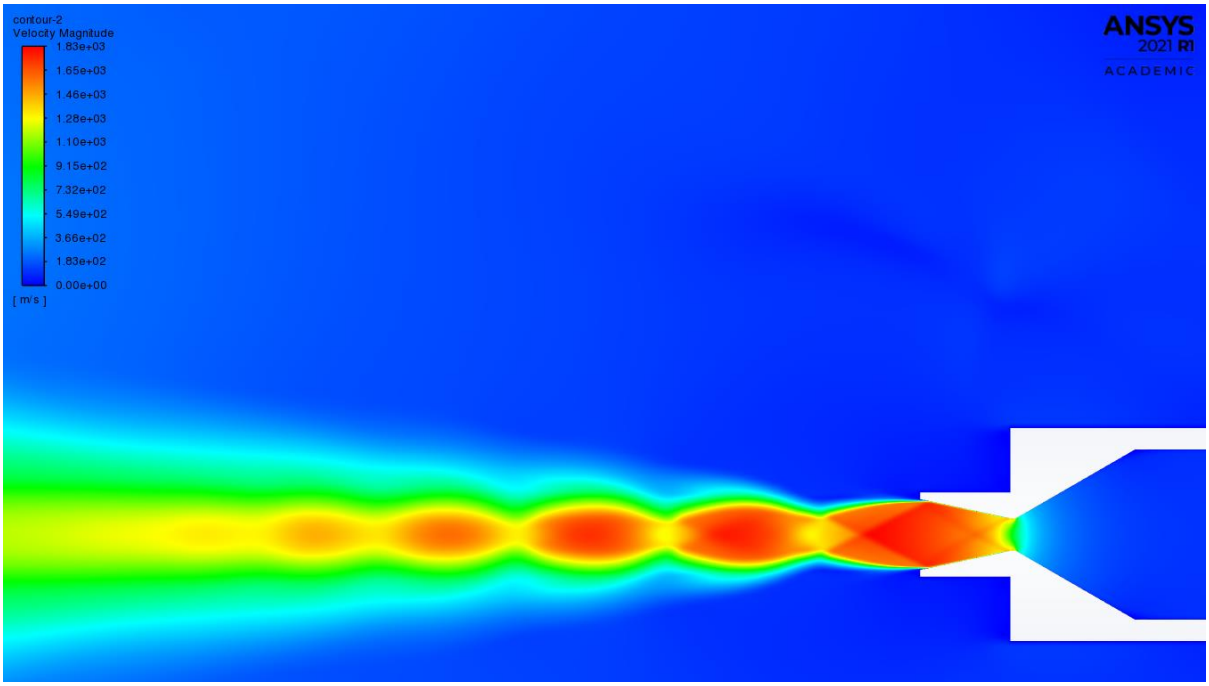

Fig. 35 - Velocity magnitude

The velocity magnitude contour looks according to expectations. The velocity at the nozzle exit area is 1826 m/s. This unfortunately means, that the specific impulse of the engine is roughly 186 seconds, which is lower than the estimated value from early calculations.

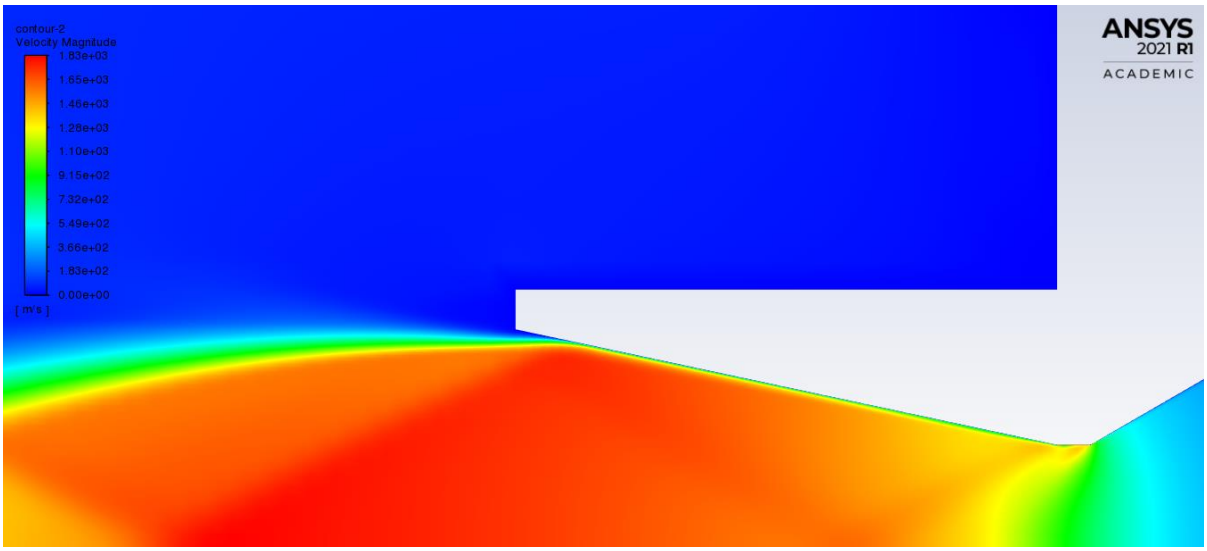

Fig. 36 - flow separation detail

As seen in Fig. 36, it seems the desire for overexpanded nozzle fired back, as the flow separation occurs just ahead of the nozzle end. While it is not a critical issue (especially at the stage of numerical simulations), the real engine should have either shorter divergent section of the nozzle, or smaller angle in order to decrease the nozzle exit area and optimize the performance.

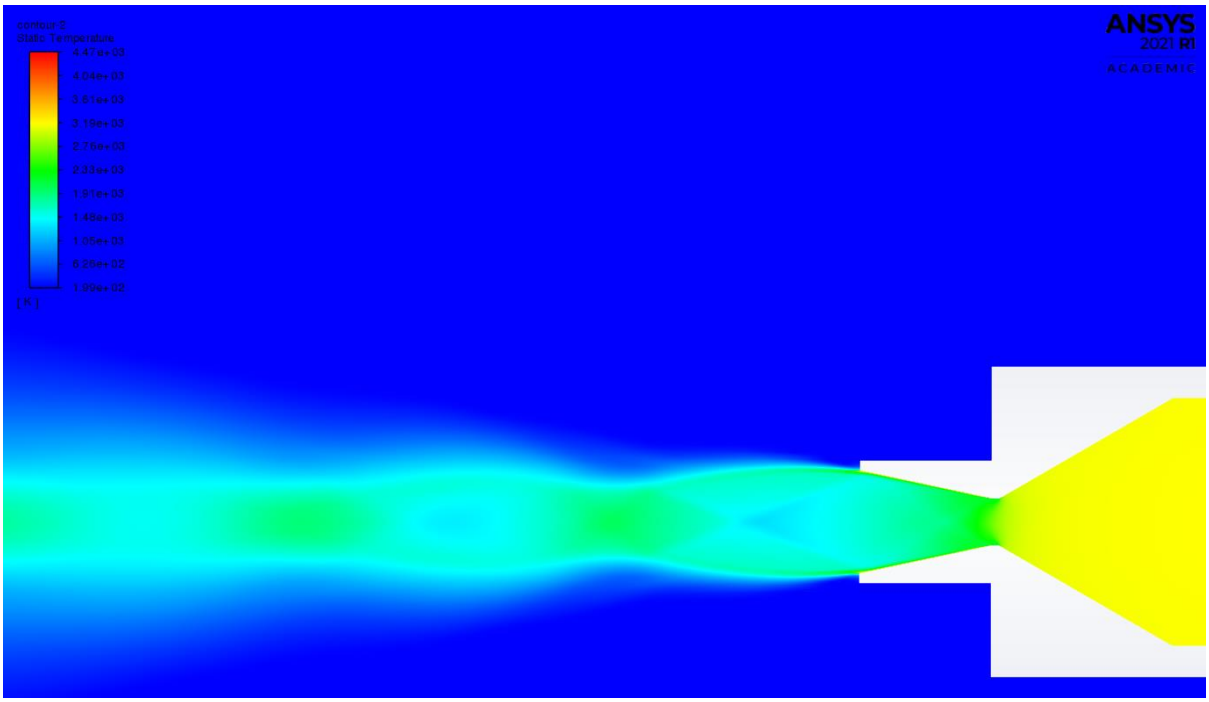

Fig. 37 - Static temperature

The temperature in the chamber equals the desired temperature of 3 200 K.
The temperature at the nozzle throat area is 2846 K, which is slightly less than precalculated temperature of 2933,75 K.
The temperature at the nozzle exit area is 1650 K.

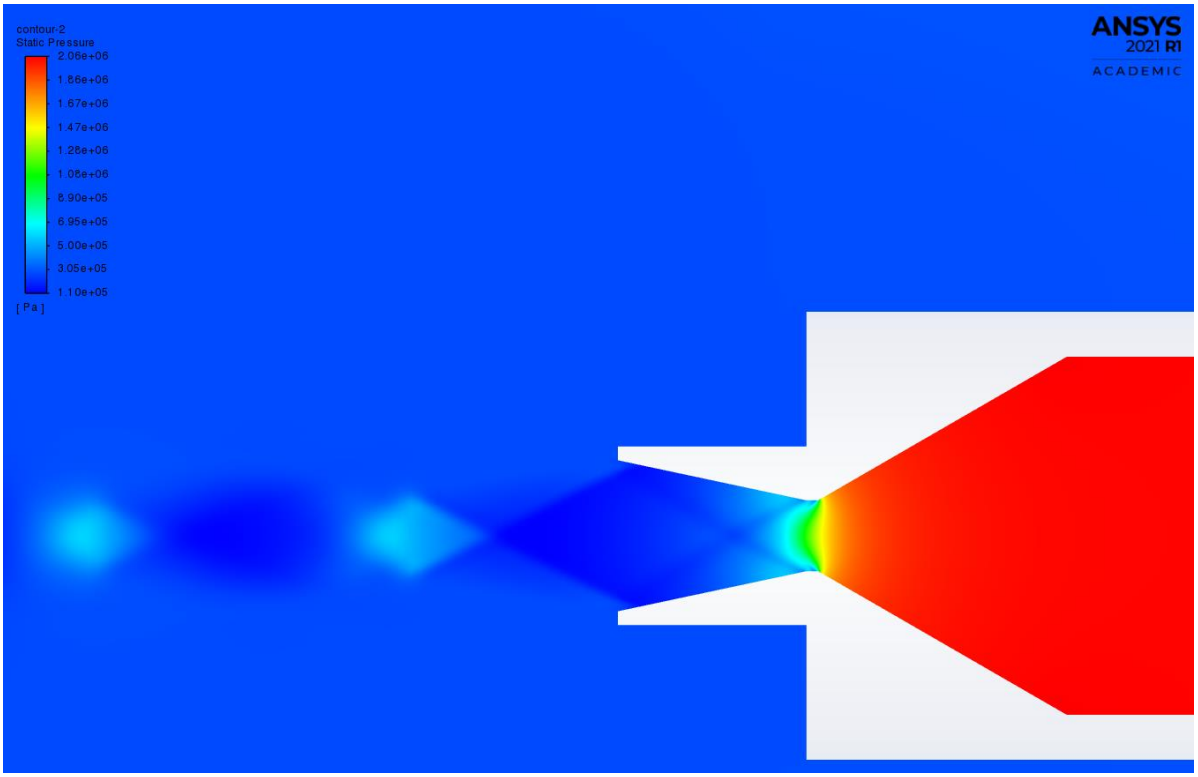

Fig. 38 - Static pressure

The initial pressure in the chamber equals the desired pressure of 2,07 MPa.

The pressure at the nozzle throat area is 1,161 MPa, which is comparable to precalculated pressure of 1,168 MPa.

The pressure at the nozzle exit area is 0,099 MPa, slightly less than the ambient pressure.

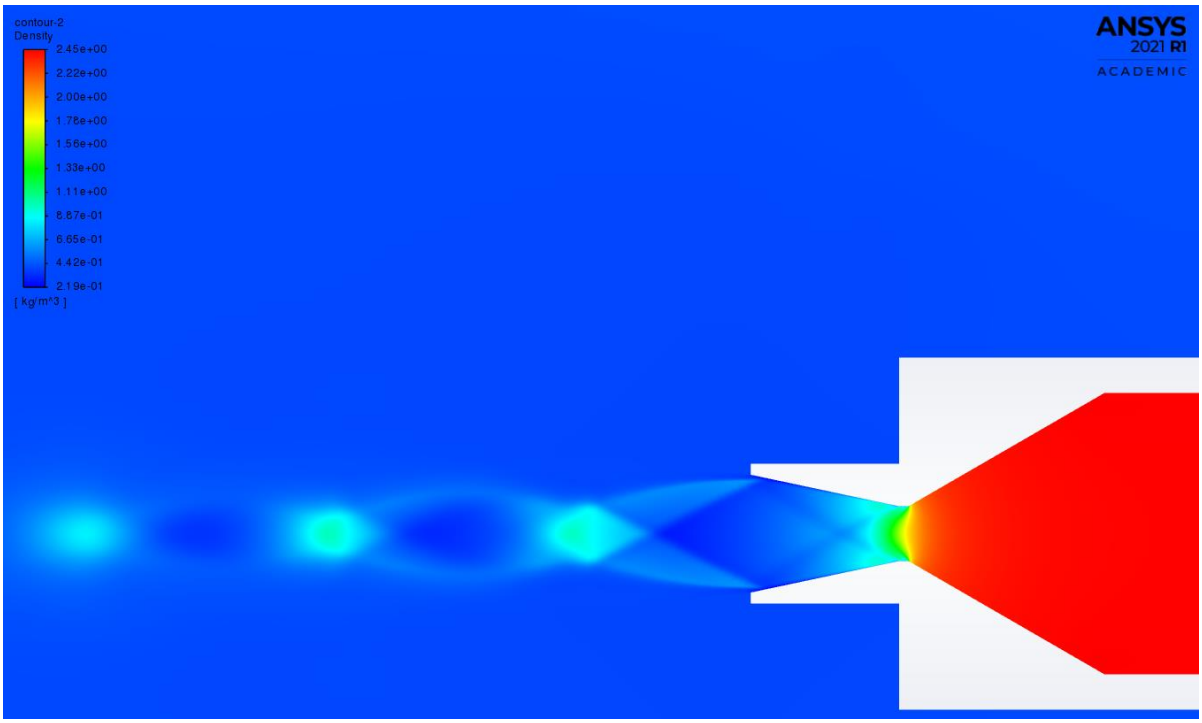

Fig. 39 - Density

3.4.2.1. Heat transfer simulation

In the second scenario I attempted to simulate the heat transfer in the cooling mechanism of the engine. For this purpose I designed a new 2D representation, that would be able to simulate the heat transfer between the hot gas and the cooling fluid, separated by the copper chamber wall.

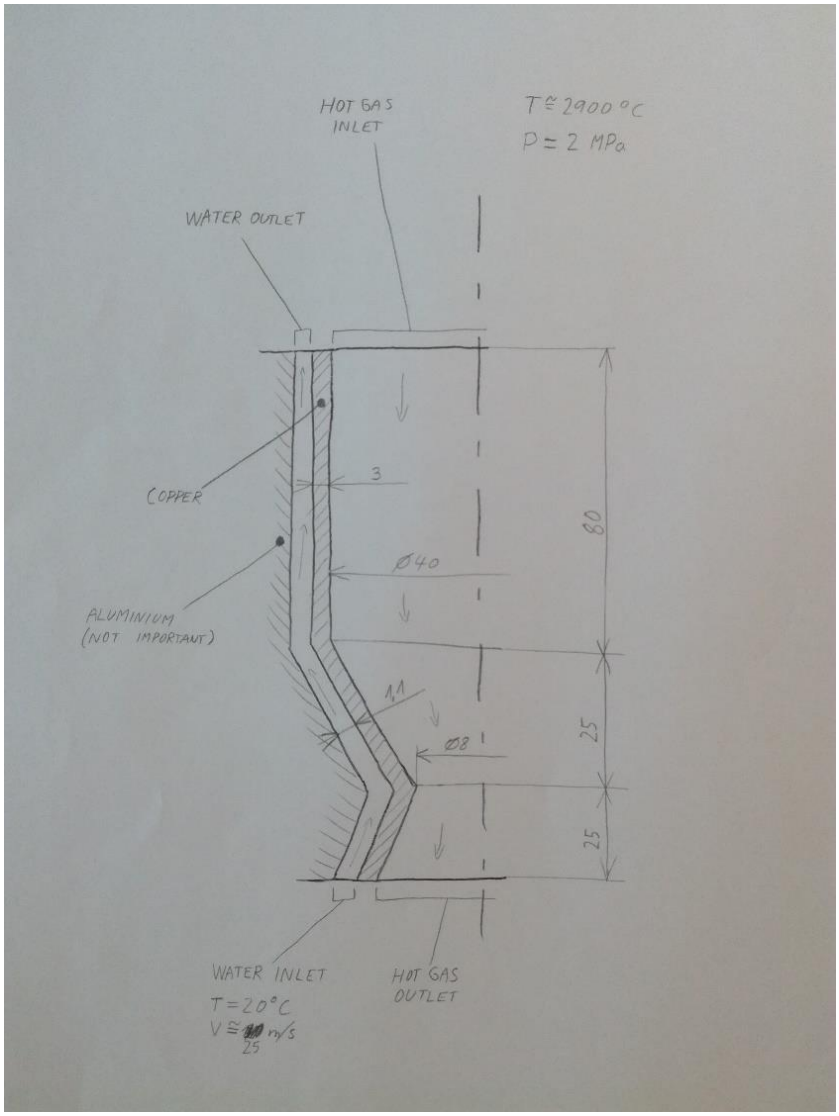

Fig. 40 - Preliminary drawing for the heat transfer numerical simulation

Once again I used the DesignModeler for this task. This case is significantly simplified compared to the CAD model (in terms of shape) to allow for much easier simulation step. According to the determined geometry I created 9 individual segments (3 for each section) and assigned their respective groups.

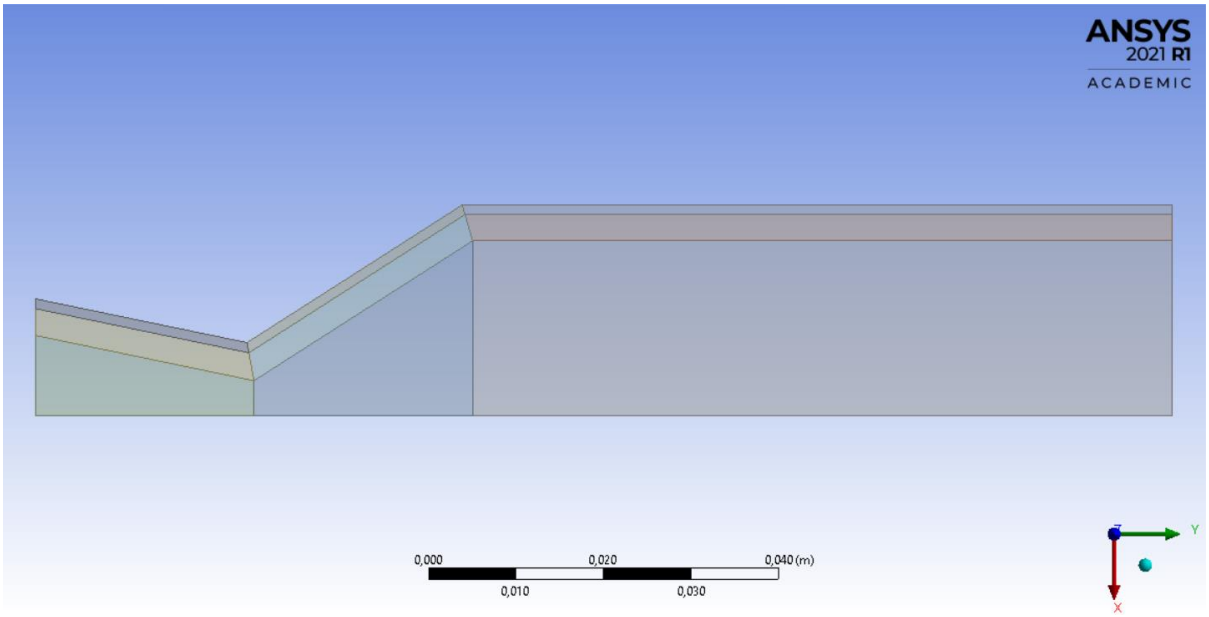

Fig. 41 - Initial segmentation

The mesh setup was pretty much a copy of the first simulation. For the edge sizing I used the near-wall model approach, and for every section I used the pure quadrilateral method of meshing. This time however, as I hadn't practical experience with this sort of simulation, I used less dense mesh. This saved a lot of time, as the simulation had to be adjusted many times before finally reaching a solved state.

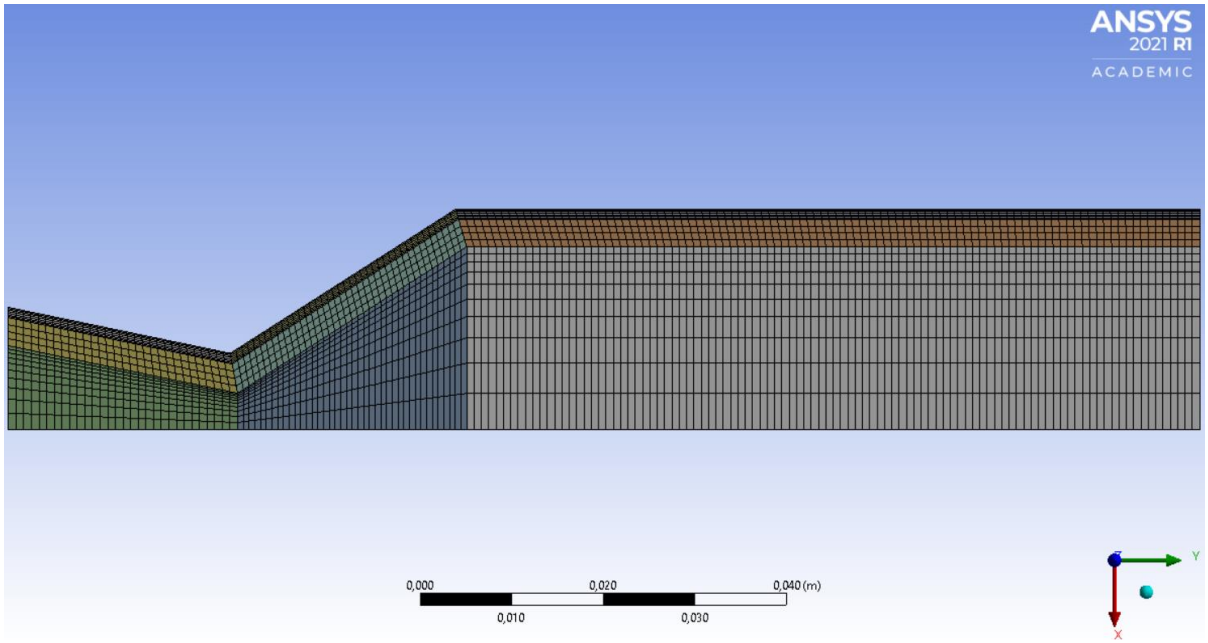

Fig. 42 – Finished mesh

For the simulation setup, in the models section, the energy equation was again turned on, and the viscous model used the realizable k-epsilon model with standard wall function of near-wall treatment as well.

For the hot gasses the air was used with the density of ideal gas and Sutherland viscosity, similarly to the first simulation. This time however, a second fluid was introduced – a liquid water with its standard properties. The water is used as a coolant. The last new substance introduced in the Solids section was the copper with its usual properties.

Then I had to specify the boundary conditions. There were multiple inlets and outlets this time. The hot gas inlet was this time treated as a velocity inlet with the value of the working pressure equalling 2 068 427 Pa, and the temperature of 3 200 K. The gas outlet was treated as a pressure outlet with the conditions of ambient atmosphere – 101,325 Pa and 300 K. The bottom wall was used as the main axis again. The second fluid inlet – the water inlet was treated as a velocity inlet as well, with the velocity of 25 m/s and temperature of 300 K. On the opposite side a water pressure outlet with the conditions of the ambient atmosphere was placed.

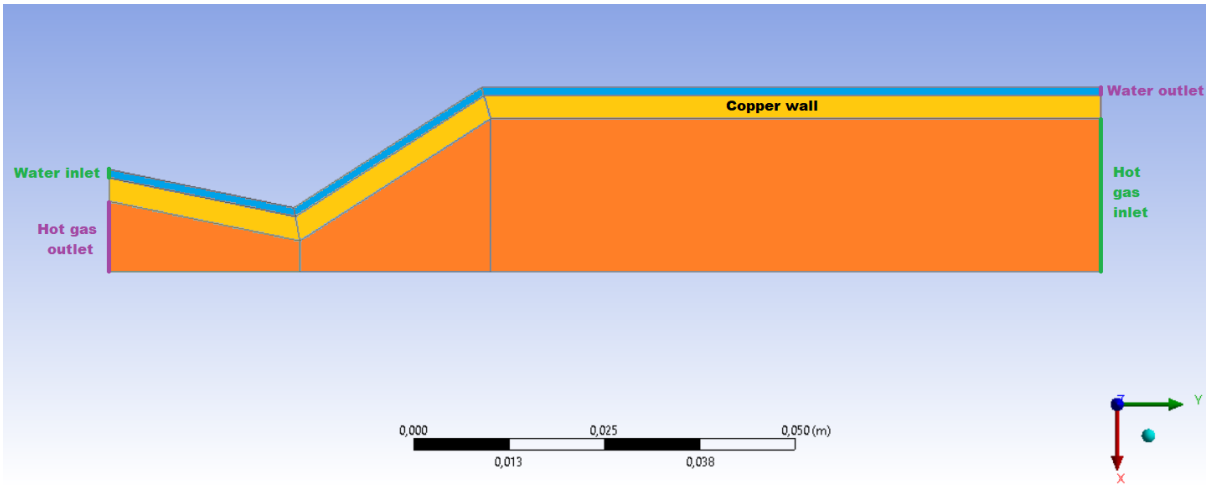

Fig. 43 - Fluid inlets and outlets

The solution method used the Pressure-Velocity Coupling with the Coupled scheme. Similar to the first simulation, the Gradient used was Least Cell Squares Based and the Flow, the Turbulent Kinetic Energy, the Turbulent Dissipation Rate and the Energy were all Second Order Upwind.

3.4.2.2. Results

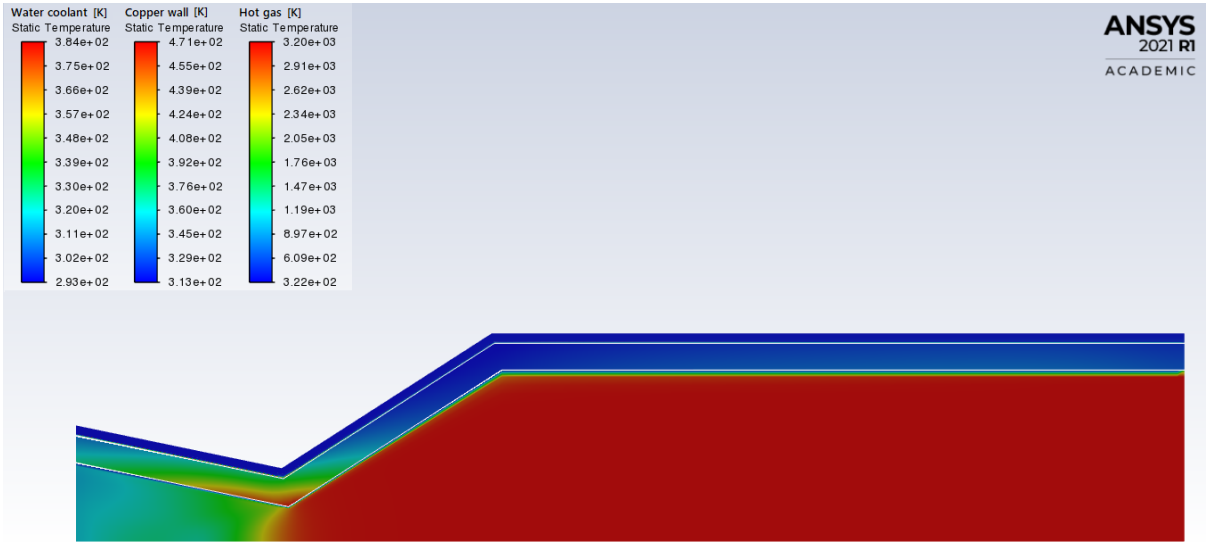

Fig. 44 - Combined temperature contours

The picture above includes combined contours of 3 different sections (coolant, copper wall and the hot gas), so the colourmap is different for each of them – pay attention to the clue in top left corner.

We can see, that the significant temperature changes occur near the nozzle throat – the temperature of the accelerating hot gas decreases, while the copper wall takes the biggest energy and its temperature therefore locally increases. The coolant temperature also increases, however it is difficult to notice in this full scale contour – will pay a closer attention in Fig. 46.

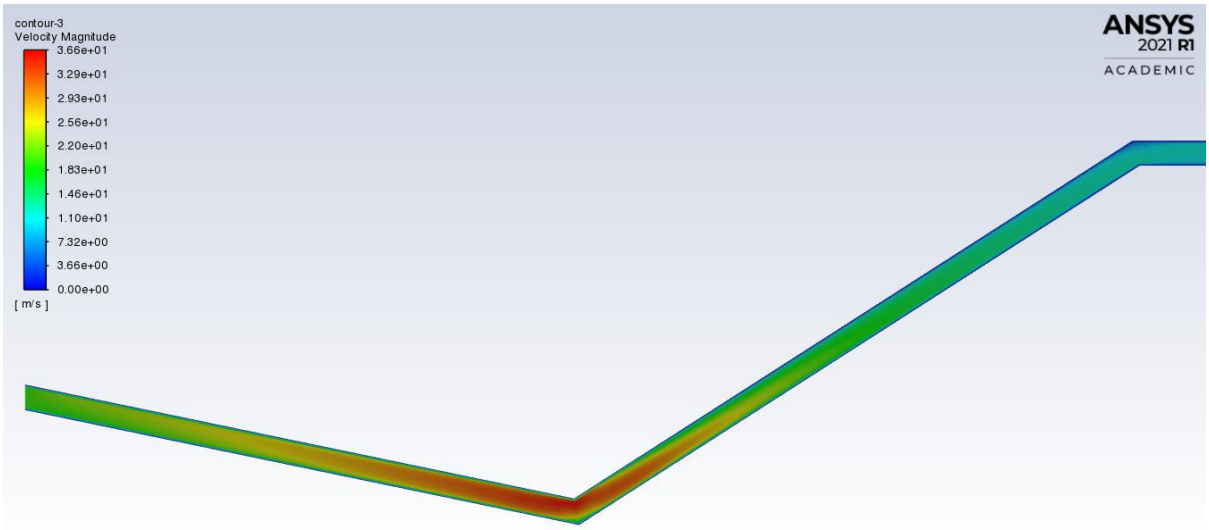

Fig. 45 - Coolant velocity detail

Following the Bernoulli's principle, in Fig. 45 the water accelerates near the nozzle throat as the diameter decreases and decelerates after passing this point. After reaching the maximal diameter, the velocity remains consistent and is close to designed 10 m/s.

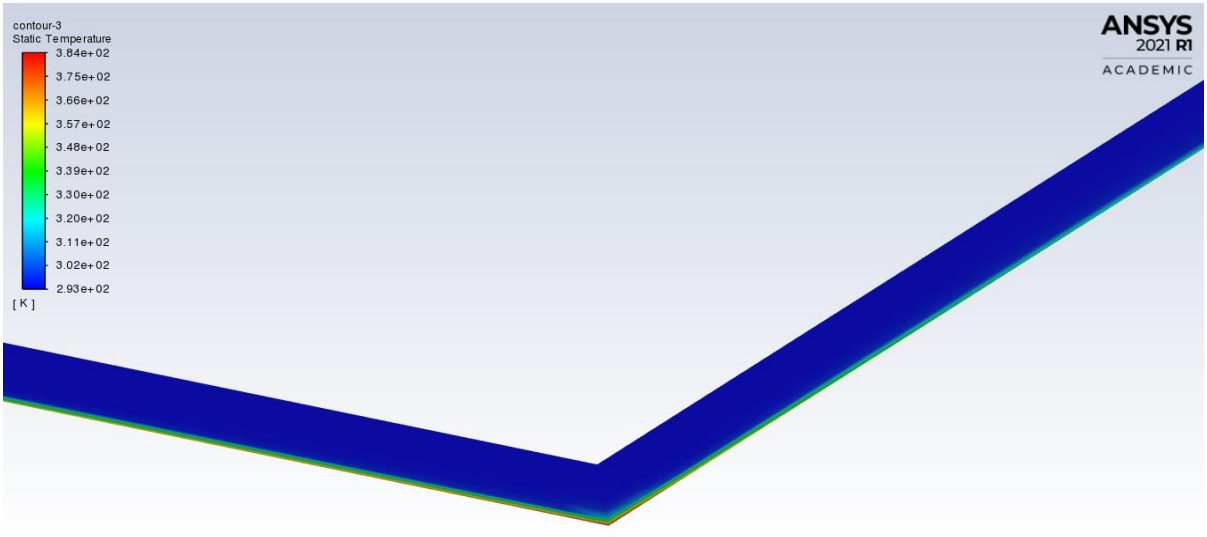

Fig. 46 - Coolant temperature detail

Taking a look at the temperature of the cooling water, there seems to be a small hotspot in the place of the minimal diameter. This is most likely the result of sudden direction changes, as the model is completely missing all radiuses and everything is made of straight lines. However considering the radiuses that will be left after the manufacturing process this should not be an issue in the real model.

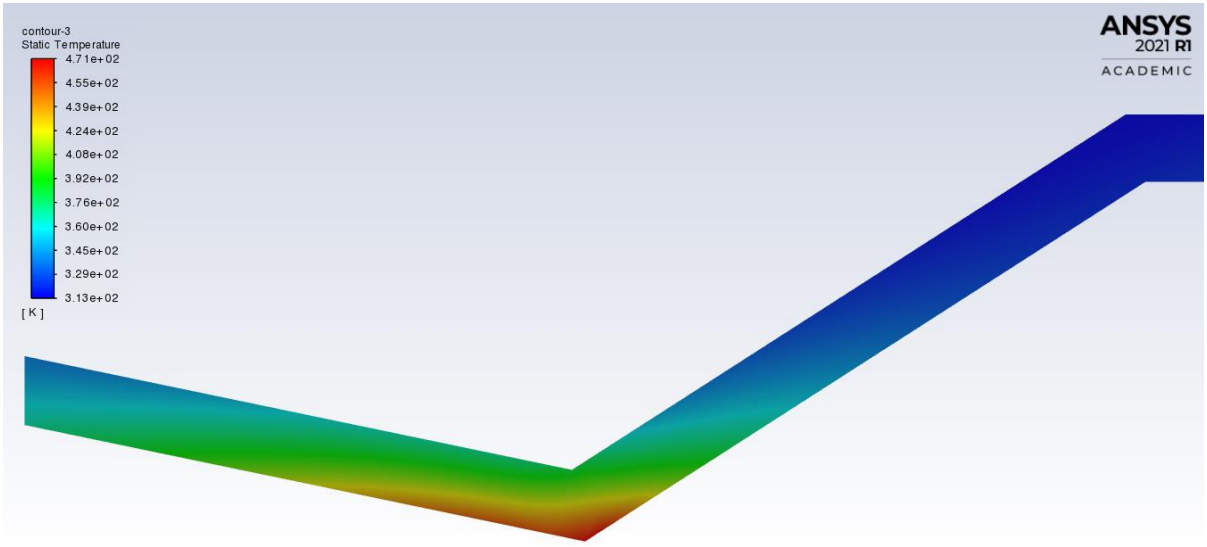

Fig. 47 - Copper wall temperature detail

The copper wall seems to be dealing with set conditions rather well. The peak temperature is 471 K (198 °C), which is very reasonable and safe temperature of this material. I was unsure, whether the wall thickness I used (3 mm) wasn't too large, but it seems to work well after all, which means that the proposed model is fail-safe (safety coef. = 3,7) and non-overheating.

3.5. Measuring apparatus

The last part of this thesis is a hypothetical measuring apparatus for the designed engine. First let's take a look at available options:

3.5.1. Orientation

1) Vertical, "pointy end down"

Widely used option, especially for solid fuel motor tests. It is simplest to install, as the force from the tested device pushes whole apparatus towards the ground. Also all the hot gasses are ejected high into the air, reducing the necessary safe space. However, this is not the most desired orientation for liquid engines, as the propellant accumulating in the combustion chamber can lead to a hard start (overpressure condition during the rocket engine ignition) and can damage or destroy the engine.

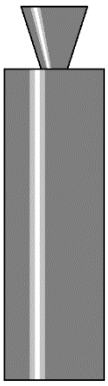

Pros:

- Simple to install
- Minimal safe space

Cons:

- Significant potential danger of a hard start

2) Horizontal

Second option is a horizontally placed engine. Very common especially for large amateur solid fuel motors. Somewhat simple to install, but requires relatively large area in the direction of exhaust plumes. The hazard of a hard start is still present for liquid engines, however is smaller compared to the first vertical option.

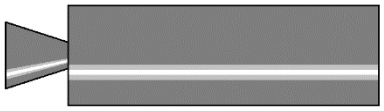

Pros:

- Somewhat simple to install
- Small risk of a hard start

Cons:

- Requires some safe space

3) Vertical, "pointy end up"

The last, most natural option. The nozzle is pointed down as is usual for rockets, also poses minimal risk of a hard start. The downside is that the apparatus has to be secured to the ground to counter the lift forces from the engine. Also as the nozzle is pointed towards the ground, the flame divertor is needed as well as some safe space.

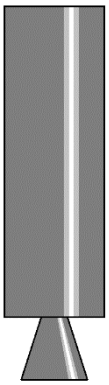

Pros:

- Natural orientation
- Minimal risk of a hard start

Cons:

- Has to be secured to the ground
- Requires flame deflector

From the available options I would most likely go with the horizontal version, which is a good compromise between simplicity if the installation and simplicity of safety precautions. The second choice would definitely be the vertical – nozzle down version.

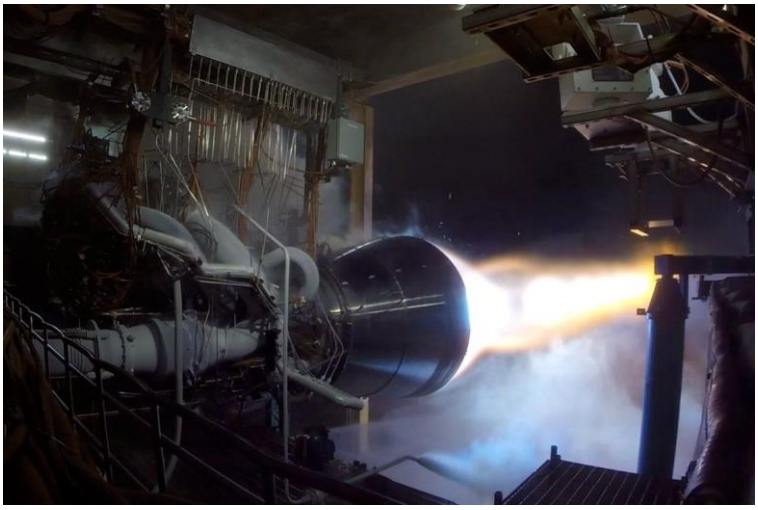

Fig. 48 – Professional liquid engine test stand [21]

3.5.2. Measurement system

For the thrust measurement of the horizontally placed rocket engine there are two main options to choose from:

1) Via a standard load cell
2) Via linear measuring system

The load cell reads the force directly – converts the force into the electric signal that can be interpreted according to the calibration. Meanwhile the linear measurement system takes advantage of a linear spring (spring with constant diameter) with its deformation proportional to the applied force. The deformation is measured via the linear measuring system and then converted into readable electric signal as well.

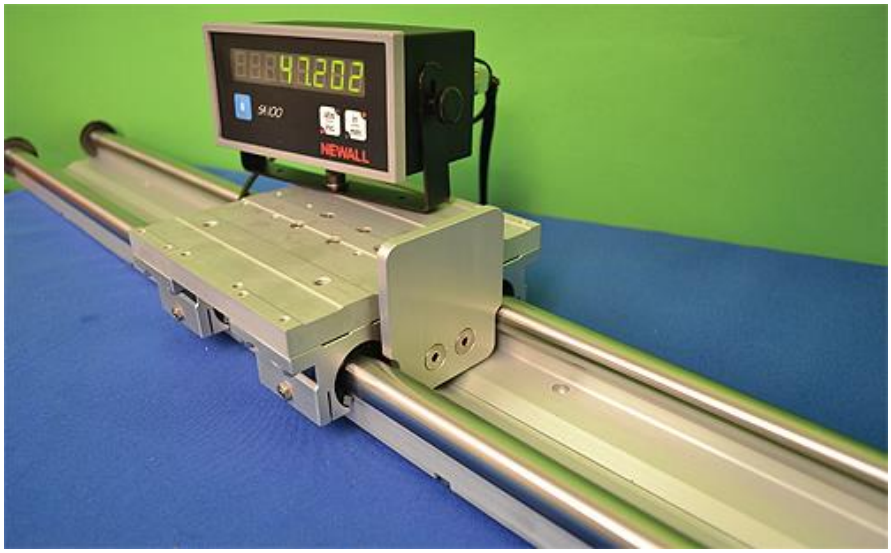

Fig. 49 - Example of a linear measuring system [22]

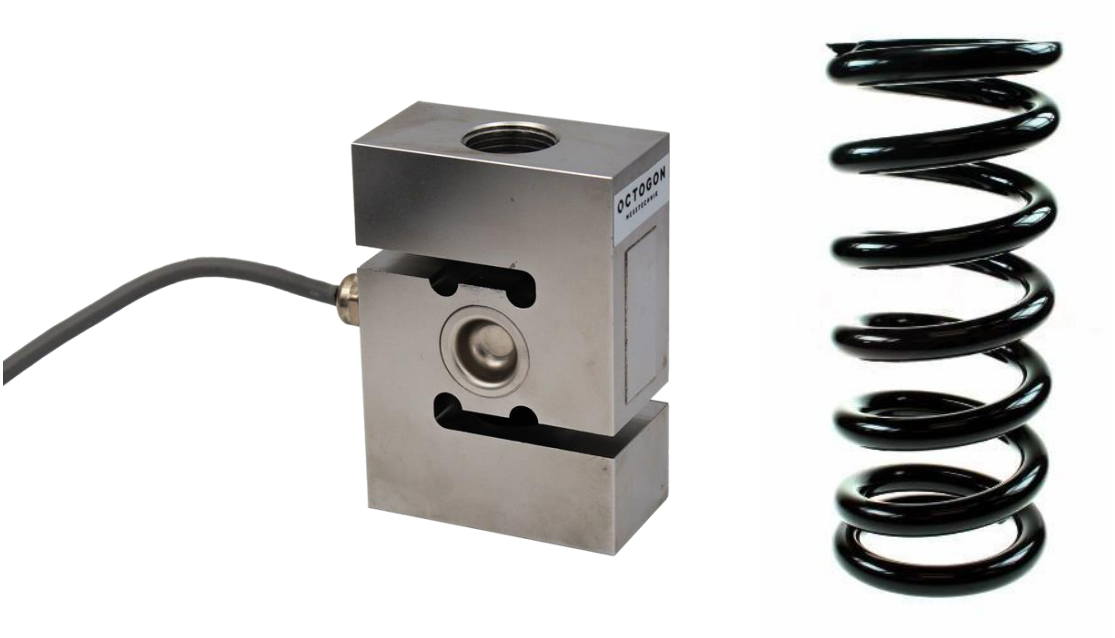

Fig. 50 - Example of a load cell and linear spring [23];[24]

3.5.3. Measuring stand requirements

Measurement range

As the engine is expected to perform around 100 N of force, there is no need to go magnitudes higher than this, unless the stand is expected to accommodate larger experimental engines in the future. Therefore I believe, that the range of 0-300 N should be more than sufficient. Eventual chance of the range should be as simple as changing the load cell (or the spring).

Measurement accuracy

Speaking of the measurement accuracy, considering this is a student's experimental engine there is no requirement for very high precision. I believe the C3 accuracy class (0,0230%) is reasonable choice for this application. This is the most common accuracy class for load cells as well. The C4 class can be used too, but I think the gains would be insignificant.

Measurement frequency

The measurement speed (the frequency of the measurement, or the sampling frequency) should correspond to the largest frequency in the set of data. If the frequency is too high, the data pack is unnecessarily large, however if the measurement frequency is too low, the undersampling occurs and the data precision is lost. That's why obeying the Nyquist frequency is important - the sampling should be at least twice the maximum signal frequency.

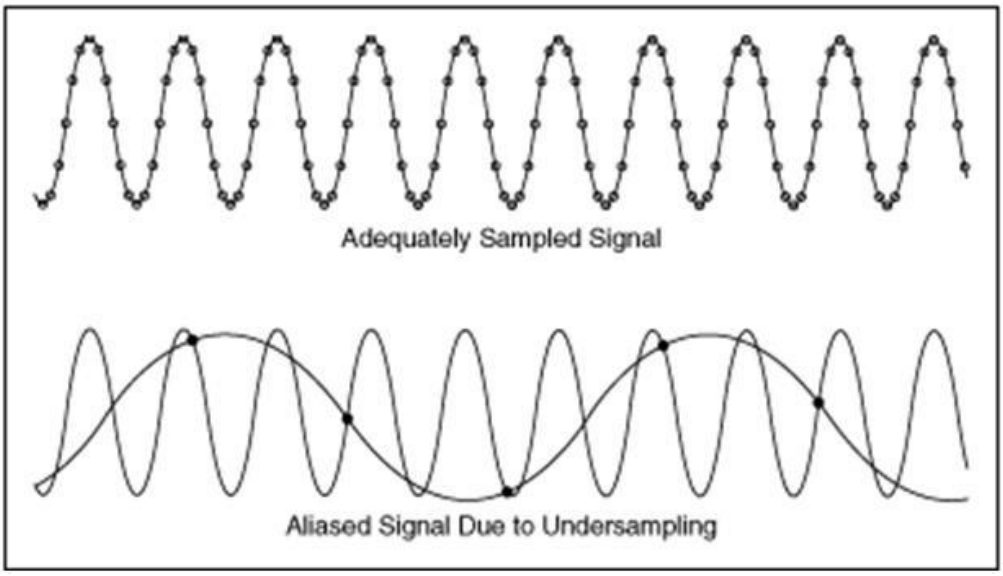

Fig. 51 - Example of the adequately sampled and the undersampled signal [25]

It is difficult to tell at what frequency will be the system oscillating, especially without having whole testing stand and the engine in hand, but from my experience based on the data measured on my Bachelor thesis solid fuel rocket motor, the sampling frequency of hundreds Hz should be reasonably big. (The mentioned motor oscillated at the frequency of roughly 80 Hz, so few hundreds Hertz should be appropriate for engine of similar size).

Propellant delivery

This engine is designed to be pressure fed – this means, that the fuel and the oxidizer are transported into the engine by the excessive pressure in the tanks. This is the simplest way of propellant delivery, the complex modern engines use pumps and turbines that are parts of large combustion cycle.

For this specific engine, the pressure feeding system can be quite simple – the oxygen and nitrogen can be stored in standard pressure vessels, while the liquid fuel can use some simple custom tank. Its size depends on the expected burn duration – this engine consumes 18,55 g/s of fuel, for a 10 seconds burn a small tank of 200 ml capacity is sufficient. A 1L tank could feed the engine for almost 54 seconds. Since this engine is regeneratively cooled, it can theoretically work for unlimited time, assuming there is enough propellant.

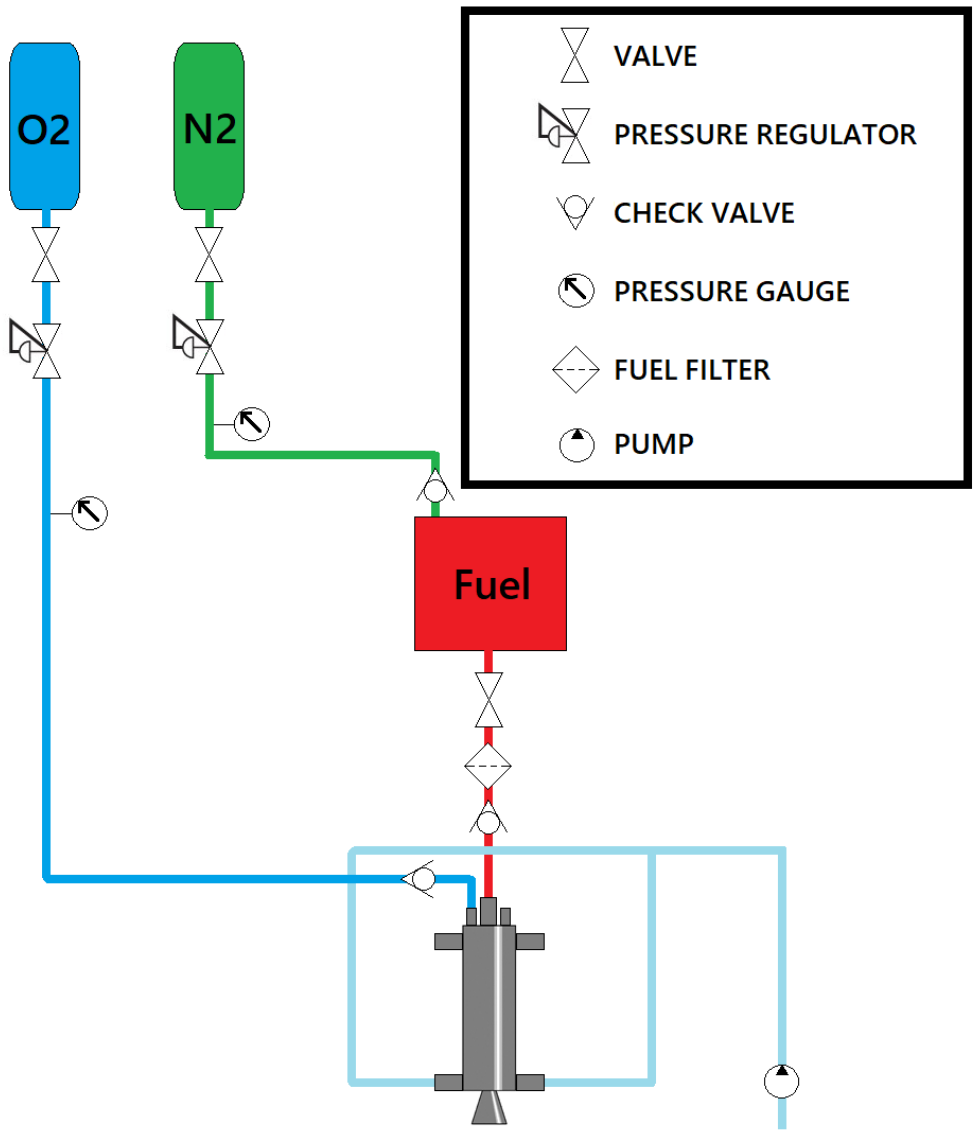

Fig. 52 - Schematic diagram of the pressure feed system

Safe space

The engine itself is 0,238 m high (or long if in horizontal orientation). My healthy estimation is, that whole testing apparatus (including the propellant storage and delivery system) could take 4 to 6 m^2 of land space. The whole safety area should be extended in the direction of the exhaust plume. Based on my own experience with amateur rocket motor/engine tests I believe that absolutely minimal size of the safe space area should be at least 20 m long and 4 m wide. By this area it is meant an open space with absolutely no objects or creatures at any point of the test. The personnel shall be advised to stay ”behind” the test stand to minimise the risk of injury from potential hazards. This is assuming all present personnel is hidden behind hard, heavy and impenetrable safety barriers as well.

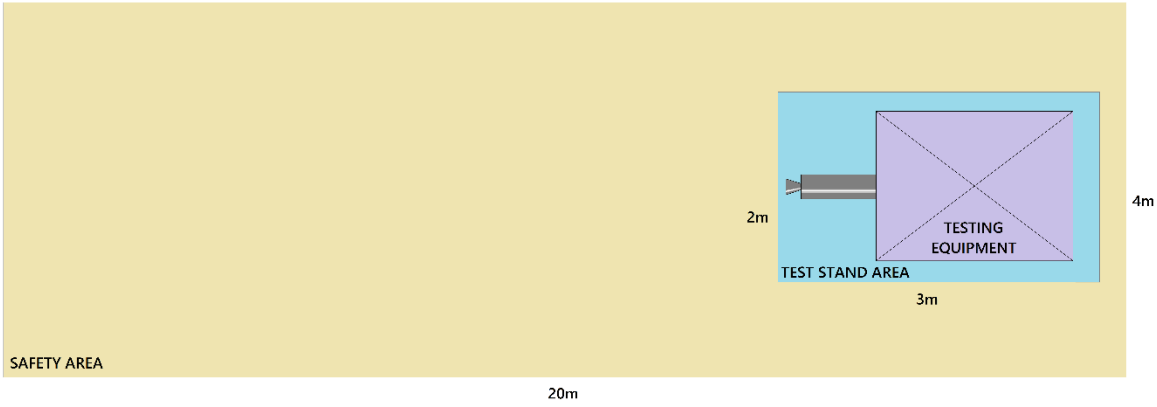

Fig. 53 - Visual estimation of the necessary space

3.6. Conclusion

In this Master thesis I calculated, 3D-modelled and numerically verified a small experimental liquid fuel rocket engine with regeneratively cooled nozzle. A quick look at a potential test stand was taken as well. According to performed numerical simulations it is safe to declare, that the engine is designed correctly and if built, should perform as desired. Although this project was purely theoretical due to COVID-19 pandemic restrictions, I strongly hope, that in the future some aerospace student may continue in this project, do some improvements to it and most importantly build and test the engine.

Nomenclature

F = force [N]

m = mass [kg]

g = standard gravitational constant [9,81 m/s^2]

T = temperature [K]

a = acceleration [m/s^2]

u; v = velocity [m/s]

I_{sp} = specific impulse [s]

t = time [s]

p = pressure [Pa]

R = universal gas law constant [8314,5 J/kmol·K]

γ = isentropic expansion factor [-]

c_p = specific heat of the gas at constant pressure [J/kg·K]

c_v = specific heat of the gas at constant volume [J/kg·K]

D; d = diameter [mm]

L = length [mm]

n = quantity [-]

ρ = density [kg/m^3]

A; S = area [m^2]

o = perimeter [mm]

k = ratio of specific heats; safety factor [-]

r = radius [mm]

σ = normal stress [Pa]

τ = shear stress [Pa]

γ = ratio of gas specific heats [-]

Abbreviations

NASA	= National Aeronautics and Space Administration
ESA	= European Space Agency
SpaceX	= Space Exploration Technologies Corporation
SRB	= solid rocket booster
RP-1	= kerosene (rocket propellant-1; redefined petroleum-1)
LOX	= liquid oxygen
HTPB	= hydroxyl-terminated polybutadiene monomer
BATES	= ballistic test and evaluation system
PVC	= polyvinyl chloride
CAD	= computer aided design
KNO_3	= potassium nitrate
CTU	= Czech Technical University in Prague

List of pictures

List of tables

List of literature

[1] Braeunig.us. (2021). *Basics of Space Flight: Rocket Propulsion*. [online] Available at: http://www.braeunig.us/space/propuls.htm [Accessed 25 May. 2021].

[2] Force diagram for rocket engine thrust. (2009). [image] Available at: https://en.wikipedia.org/wiki/File:Rocket_thrust.svg [Accessed 26 May 2021].

[3] Sutton, G. and Biblarz, O. (2017). *Rocket propulsion elements*. New York: John Wiley & Sons, p.28.

[4] En.wikipedia.org. (2021). *Tsiolkovsky rocket equation*. [online] Available at: https://en.wikipedia.org/wiki/Tsiolkovsky_rocket_equation [Accessed 23 Jun. 2021].

[5] NASA's Space Shuttle Endeavour. (n.d.). [image] Available at: http://www.whoinventedthis.org/who-invented-the-space-shuttle/ [Accessed 22 Apr. 2021].

[6] Virgin Galactic's SpaceShipTwo. (n.d.). [image] Available at: https://spaceflightnow.com/2018/05/30/virgin-galactics-spaceshiptwo-completessecond-powered-test-flight/ [Accessed 22 April 2021].

[7] A de Laval nozzle, showing approximate flow velocity increasing from green to red in the direction of flow. (2005). [image] Available at: https://en.wikipedia.org/wiki/Rocket_engine_nozzle#/media/File:De_laval_nozzle.svg [Accessed 8 Jul. 2021].

[8] Nozzle de Laval diagram. (2008). [image] Available at: https://en.wikipedia.org/wiki/File:Nozzle_de_Laval_diagram.svg [Accessed 14 Apr. 2019].

[9] The four expansion regimes of a de Laval nozzle. (2009). [image] Available at: https://en.wikipedia.org/wiki/Rocket_engine#/media/File:Rocket_nozzle_expansion.svg [Accessed 15 Jun 2021].

[10] En.wikipedia.org. (2021). Liquid propellant rocket. [online] Available at: https://en.wikipedia.org/wiki/Liquid-propellant_rocket [Accessed 2 Jun. 2021].

[11] Goddard and rocket (n.d.). [image] Available at: https://upload.wikimedia.org/wikipedia/commons/7/7c/Goddard_and_Rocket.jpg [Accessed 22 Apr. 2021].

[12] En.wikipedia.org. (2021). Wernher von Braun. [online] Available at: https://en.wikipedia.org/wiki/Wernher_von_Braun [Accessed 21 May. 2021].

[13] V-2 Rocket (n.d.). [image] Available at: https://upload.wikimedia.org/wikipedia/commons/6/66/La2-v2.jpg [Accessed 7 May. 2021].

[14] Britannica. (2021). Liquid propellant rocket engines. [online] Available at: https://www.britannica.com/technology/rocket-jet-propulsion-device-and-vehicle/Liquid-propellant-rocket-engines [Accessed 9 Jun. 2021].

[15] Example of full flow staged rocket cycle (n.d.). [image] Available at: https://en.wikipedia.org/wiki/Staged_combustion_cycle#/media/File:Staged_combustion_rocket_cycle.svg [Accessed 18 Jul. 2021].

[16] J. KRZYCKI, Leroy. How to design, build and test small liquid-fuel rocket engines. 2nd ed. United States of America, 1967. ISBN 9600-1980-4., p.8.

[17] Flame temperature vs. the chamber pressure [image] J. KRZYCKI, Leroy. How to design, build and test small liquid-fuel rocket engines. 2nd ed. United States of America, 1967. ISBN 9600-1980-4., p.9.

[18] Flame temperature vs. the mixture ratio [image] J. KRZYCKI, Leroy. How to design, build and test small liquid-fuel rocket engines. 2nd ed. United States of America, 1967. ISBN 9600-1980-4., p.10.

[19] Performance of hydrocarbon fuels with gaseous oxygen [image] J. KRZYCKI, Leroy. How to design, build and test small liquid-fuel rocket engines. 2nd ed. United States of America, 1967. ISBN 9600-1980-4., p.11.

[20] Nozzle parameters for various chamber pressures [image] J. KRZYCKI, Leroy. How to design, build and test small liquid-fuel rocket engines. 2nd ed. United States of America, 1967. ISBN 9600-1980-4., p.16.

[21] Professional liquid fuel engine test stand (n.d.). [image] Available at: https://hips.hearstapps.com/pop.h-cdn.co/assets/17/42/1508508230-dmijjxsv4aajc1g.jpg [Accessed 12 Jul. 2021].

[22] Example of a linear measuring system (n.d.). [image] Available at: https://3yq5q42rw3z48qnbj46yehrx-wpengine.netdna-ssl.com/wp-content/uploads/2012/09/SMI-Linear-Digital-Measuring-Device.jpg [Accessed 12 Jul. 2021].

[23] Example of a load cell and linear spring (n.d.). [image] Available at: https://www.octogon.org/images/wagezelle/s_typ_waegezelle.png [Accessed 12 Jul. 2021].

[24] Example of a load cell and linear spring (n.d.). [image] Available at: https://cdn.shopify.com/s/files/1/0508/9312/7879/products/bc_spring_25.jpg [Accessed 12 Jul. 2021].

[25] Example of the adequately sampled and the undersampled signal (n.d.). [image] Available at: https://turbomass.files.wordpress.com/2019/04/w.jpg [Accessed 12 Jul. 2021].